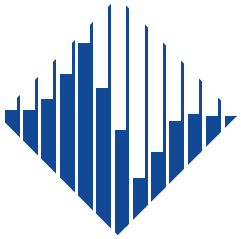

PACIFIC EARTHQUAKE ENGINEERING
RESEARCH CENTER

Selection of Random Vibration Procedures for the NGA-East Project

Albert Kottke
Norman A. Abrahamson
David M. Boore
Yousef Bozorgnia
Christine Goulet
Justin Hollenback
Tadahiro Kishida
Armen Der Kiureghian
Olga-Joan Ktenidou
Nicolas Kuehn
Ellen M. Rathje
Walter J. Silva
Eric Thompson
Xiaoyue Wang

PEER Report No. 2018/05
Pacific Earthquake Engineering Research Center
Headquarters at the University of California, Berkeley

November 2018

PEER 2018/05
November 2018

Disclaimer

The opinions, findings, and conclusions or recommendations expressed in this publication are those of the author(s) and do not necessarily reflect the views of the study sponsor(s), the Pacific Earthquake Engineering Research Center, or the Regents of the University of California.

Selection of Random Vibration Procedures for the NGA-East Project

Albert Kottke
Norman A. Abrahamson
David M. Boore
Yousef Bozorgnia
Christine Goulet
Justin Hollenback
Tadahiro Kishida
Armen Der Kiureghian
Olga-Joan Ktenidou
Nicolas Kuehn
Ellen M. Rathje
Walter J. Silva
Eric Thompson
Xiaoyue Wang

PEER Report No. 2018/05
Pacific Earthquake Engineering Research Center
Headquarters at the University of California, Berkeley
November 2018

ABSTRACT

Pseudo-spectral acceleration (PSA) is the most commonly used intensity measure in earthquake engineering as it serves as a simple approximate predictor of structural response for many types of systems. Therefore, most ground-motion models (GMMs, aka GMPEs) provide median and standard deviation PSA using a suite of input parameters characterizing the source, path, and site effects. Unfortunately, PSA is a complex metric: the PSA for a single oscillator frequency depends on the Fourier amplitudes across a range of frequencies. The Fourier amplitude spectrum (FAS) is an appealing alternative because its simple linear superposition allows effects to be modeled as transfer functions. For this reason, most seismological models, i.e., the source spectrum, are developed for the FAS. Using FAS in conjunction with random-vibration theory (RVT) allows GMM developers to superimpose seismological models directly, computing PSA only at the end of the process. The FAS-RVT-PSA approach was first used by the Hollenback et al. team in their development of GMMs for the Next Generation Attenuation Relationships for Central & Eastern North-America (NGA-East) project (see Chapter 11 of *PEER Report No. 2015/04*). As part of the NGA-East project to support the Hollenback et al. team and similar efforts, the current report summarizes a systematic processing algorithm for FAS that minimizes computational requirements and bias that results from the RVT approximation for median GMM development.

ACKNOWLEDGMENTS

This study was sponsored by the Pacific Earthquake Engineering Research Center (PEER) as part of the NGA-East research project, and was funded by the U.S. Nuclear Regulatory Commission (NRC), the U.S. Department of Energy (DOE), and the Electric Power Research Institute (EPRI), with participation of the U.S. Geological Survey (USGS).

Any opinions, findings, and conclusions or recommendations expressed in this material are those of the authors and do not necessarily reflect those of the sponsoring agencies, PEER, or the Regents of the University of California.

CONTENTS

LIST OF TABLES

LIST OF FIGURES

1 Introduction

Random-vibration theory (RVT) is a method to statistically represent earthquake ground motions that allows for the calculation of the expected time-domain peak value with one calculation. It has been used by seismologists and engineers for decades for a wide range of applications (e.g., Hanks and McGuire [1981], Boore and Joyner [1984], Campbell [2003], and Rathje et al. [2005]). In the context of quantifying ground motions, RVT is used to compute pseudo-spectral acceleration (PSA), starting from a statistical representation of the Fourier amplitude spectrum (FAS) and an associated measure of duration. Pseudo-spectral acceleration is the most commonly used metric in earthquake engineering. Because it is a simple predictor of structural response for many types of systems, ground motion models (GMMs) have been developed for PSA; however, PSA is a highly nonlinear metric. It depends on various bandwidths captured by different single-degree-of-freedom (SDOF) systems, which makes it difficult to translate seismological effects directly to PSA. Thus, most seismological models have been developed for FAS, one of the fundamental building blocks of the frequency domain representation of ground motions. Using FAS in conjunction with the RVT process allows GMM developers to superimpose various seismological models directly and computes PSA only at the end of the process. Although this process cannot account for all the time-dependent effects of recorded ground motions, it presents the advantage of relative simplicity for integrating complex seismological models into median PSA computations.

The RVT approach was considered for the development of GMMs for the Next Generation Attenuation Relationships for Central & Eastern North-America (NGA-East) project. This report provides an overview of the basic concepts of the RVT method, discusses previously proposed methods, and summarizes methodologies adopted for use by the NGA-East project.

1.1 MOTIVATION AND CONSTRAINTS

Traditional GMMs are used to compute the expected PSA—as well as other intensity measures (IMs)—for a given scenario event (defined by an earthquake magnitude and source–site distance measures). The response spectrum was selected as the IM of choice because it is generally a good predictor of the dynamic response of a wide range of structures. Each frequency of the response spectrum corresponds to the peak time-domain response of a SDOF system with a specific natural period and damping. The SDOF response depends on the frequency content and timing (or phasing) characteristics of the ground motions. The response is largely controlled by

amplitudes in the frequency range near to and lower than the natural frequency of the SDOF system. Thus, for a high-frequency system, the oscillator response is dependent on nearly all of the frequency content of the ground motion. As a result, changes in the ground-motion response spectrum are dependent on the frequency content of the input motion (i.e., spectral shape). Spectral shape refers to the trace of any amplitude metric as a function of frequency. This report applies this concept of spectral shape to both PSA and FAS. The dependence on spectral shape on the oscillator response complicates the development and functional form of GMMs.

The FAS has one main advantage over the PSA spectrum: the amplitude at each frequency is independent of the amplitudes of adjacent frequencies. The same site amplification, distance attenuation, site attenuation, etc., is applicable to any motion regardless of the spectral shape. The primary disadvantage of the FAS is that it is not a useful IM for engineering design. The RVT solves this problem by providing a method to compute the expected peak response in the time domain (e.g., PGA, PGV, etc.). By coupling RVT with the SDOF transfer function, it becomes possible to calculate the expected acceleration response spectrum that corresponds to the FAS. The GMM development can therefore be completed in FAS space—where many processes are linear—with the PSA computed using RVT theory models.

The RVT relies on extreme value statistics, which describe the distribution of peak values of the underlying time-varying seismogram. Because of complexities inherent in a seismogram, there is no exact solution. Instead, there are a number of proposed solutions, each with their own advantages and disadvantages. The NGA-East project required that the RVT procedure provides accurate results over the widest frequency range possible. The NGA-East GMMs were developed for reference-rock site conditions that were paired with site-amplification models to address site response. To maintain consistency between the GMM and site-amplification model development, the selected RVT approach should also be applicable to site response analyses.

This report is structured as follows: (1) it presents an overview of the RVT approach; (2) discusses the selection of peak factors to use for the GMM development application; (3) introduces a down-sampled orientation-independent FAS referred to as the effective amplitude spectrum (EAS); and (4) discusses alternative duration models that are consistent with the RVT process. The down-sampled smoothed EAS was applied and included as data products for the NGA-East, NGA-West2, and NGA-Sub databases.

2 Random-Vibration Theory: Fundamentals

In practice, RVT can be separated into a theoretical framework that relates the frequency content and duration of the motion to the distribution of peak time-domain response; empirical corrections are used to improve the accuracy of RVT where assumptions begin to limit the methodology. This chapter discusses the methodology used to characterize the ground motion and calculate the peak-time response.

2.1 CHARACTERIZATION OF RANDOM-VIBRATION THEORY GROUND MOTION

In RVT, the ground motion is characterized the power spectral density (PSD). For time varying signal $x(t)$, the $\mathrm{PSD}(f)$ can be computed by:

$$\mathrm{PSD}(f) = \left[X(f)\right]^2 / D \tag{2.1}$$

where $X(f)$ is the FAS, and D is the ground-motion duration (see Section 2.3). Seismology has typically separated the frequency content [i.e., $X(f)$] and the duration instead of being combined into the PSD. If an RVT motion is defined as the average of a set of time series, then the FAS should correspond to the mean power, which is computed by the mean value of the squared Fourier amplitudes [Boore 2003].

The frequency content may be indirectly specified by a response spectrum from which a compatible FAS is developed. While specifying the ground motion in this manner is advantageous due to the general familiarity with the response spectrum, there are challenges associated with ground-motion saturation of the SDOF transfer function. The details of this process of developing a compatible FAS from a target response spectrum is not discussed herein; more information can be found in Vanmarcke [1976], Der Kiureghian [1980], and Rathje et al. [2005].

2.2 CALCULATING THE PEAK RESPONSE

The peak factor (PF) relates the root-mean-squared response to the peak response. The following assumptions of the ground are required for the development of the PF formulations:

- They can be represented by a band-limited white Gaussian noise (amplitudes have random phases) with zero mean.
- It is a stationary stochastic process with no change in the probability distribution over the duration interval.

The ramifications of these proposed assumptions are discussed in Chapter 3.

Consider a time-varying signal $x(t)$ with its associated FAS $X(f)$: the root mean square (rms) value of the signal (x_{rms}) is a measure of the average value over a given time interval, D_{rms}, and is computed from the integral of the time series over that time interval by:

$$x_{\text{rms}} = \sqrt{\frac{1}{D_{\text{rms}}} \int_0^{D_{\text{rms}}} \left[x(t)\right]^2 dt} \tag{2.2}$$

Parseval's theorem relates the integral of a time series to the integral of its Fourier transform such that Equation (2.2) can be re-written in terms of the FAS of the signal:

$$x_{\text{rms}} = \sqrt{\frac{2}{D_{\text{rms}}} \int_0^{\infty} \left|X(f)\right|^2 df} = \sqrt{\frac{m_0}{T_{\text{rms}}}} \tag{2.3}$$

where m_0 is defined as the *zero*th moment of the FAS. The *n*th moment of the FAS is defined as:

$$m_n = 2\int_0^{\infty} (2\pi f)^n \left|X(f)\right|^2 df \tag{2.4}$$

and is used characterize the frequency content of the ground motion. The spectral motions are used to define the frequency of zero crossings (f_z) by:

$$f_z = \frac{1}{\pi}\sqrt{\frac{m_2}{m_0}} \tag{2.5}$$

and the number of zero crossings (N_z) by:

$$N_z = f_z \cdot D_{\text{gm}} = \frac{1}{\pi}\sqrt{\frac{m_2}{m_0}} \cdot D_{\text{gm}} \tag{2.6}$$

where D_{gm} is the duration of the ground motion; this is discussed in more detail in Section 2.3. Similarly, the frequency (f_e) and number (N_e) of extrema can be computed by:

$$f_e = \frac{1}{\pi}\sqrt{\frac{m_4}{m_2}} \tag{2.7}$$

$$N_e = f_e \cdot D_{\text{gm}} = \frac{1}{\pi}\sqrt{\frac{m_4}{m_2}} \cdot D_{\text{gm}} \tag{2.8}$$

2.2.1 Peak Factor Formulations

2.2.1.1 Cartwright and Longuet-Higgins [1956]

Cartwright and Longuet-Higgins [1956] (abbreviated as CLH56) studied ocean waves and developed functions to predict peak wave height based on characteristics of the wave train. Boore [1983; 2003] modified the PF equation by changing the variables to remove an integrable singularity. The resulting PF equation is:

$$\mathrm{PF} = \frac{x_{\max}}{x_{\min}} = \sqrt{2}\int_0^{\infty}\left\{1-\left[1-\varepsilon\exp\left(-z^2\right)\right]^{N_e}\right\}dz \tag{2.9}$$

where ε is defined as ratio of number of zero crossings $\left(N_z\right)$ to the number of extrema $\left(N_e\right)$:

$$\varepsilon = \frac{N_z}{N_e} + \sqrt{\frac{\left(m_2\right)^2}{m_0 \cdot m_4}} \tag{2.10}$$

The number of zero crossings and extrema are defined in Equations (2.6) and (2.8).

Equation (2.9) assumes a Poisson process in which each peak is statistically independent. For narrow-band motions (ε = 1), the distribution of peaks follow a Rayleigh distribution. For broadband motions (ε = 0), the distribution of peaks follow a Gaussian distribution.

2.2.1.2 Davenport [1964]

Davenport [1964] (abbreviated as D64) simplified Equation (2.9) to the following asymptotic form:

$$\mathrm{PF} = \frac{x_{\max}}{x_{\min}} = \sqrt{2\ln\left(N_z\right)} + \frac{0.5772}{\sqrt{2\ln\left(N_z\right)}} \tag{2.11}$$

which results in faster calculations but at the cost of decreased accuracy; see Section 2.2.2. Note: this approximation does not work if N_z is less or equal to 1.

2.2.1.3 Vanmarcke [1975]

Vanmarcke [1975] (abbreviated as V75) extended the previous PF formulations to include the potential for clustering of peak values in the time domain. This formulation no longer assumes a Poisson process with statistically independent peaks. The cumulative distribution of the peak values from Equation (29) of Vanmarcke [1975] is as follows:

$$F_x\left(x\right) = \left[1-\exp\left(-\frac{x^2}{2}\right)\right]\exp\left\{-\frac{N_z\left[1-\exp\left(-\sqrt{\frac{\pi}{x}}\cdot\delta_e\cdot x\right)\right]}{1-\exp\left(-\frac{x^2}{2}\right)}\right\} \tag{2.12}$$

where δ_e is an empirically defined factor defined as:

$$\delta_e = \delta^{1+b} \tag{2.13}$$

where δ another measure of bandwidth defined by:

$$\delta = \sqrt{1 - \frac{(m_1)^2}{m_0 \cdot m_2}} \tag{2.14}$$

and the value of b was tentatively estimated to be 0.20 based on fitting to numerical simulations. Equation (2.12) does not provide for direct calculation of the expected PF. Instead, it is possible to calculate the expected PF through first computing the analytical or numerical derivative of Equation (2.12) prior to computing the expected value of the probability density function, $[f_x(x)]$, which is defined as:

$$E[x] = \int_0^\infty x \cdot f_x(x) dx \tag{2.15}$$

However, because F_x is continuous and only non-negative, the expected value may be computed directly from F_x by[1,2]:

$$E[x] = \int_0^\infty \left[1 - F_x(x)\right] dx \tag{2.16}$$

The PF is then computed by substituting Equation (2.12) into Equation (2.16).

2.2.1.4 Der Kiureghian [1980]

Der Kiureghian [1980] (abbreviated as DK80) assessed the Davenport [1964] PF formulation and identified that the Poisson model of crossings tends to overestimate the mean and underestimate the variance of the peak. Der Kiureghian [1980] modified the Davenport [1964] asymptotic equation based on empirical data, and defined the PF as:

$$\text{PF} = \frac{x_{\max}}{x_{\text{rms}}} = \sqrt{2\ln(N_z^*)} + \frac{0.5772}{\sqrt{2\ln(N_z^*)}} \tag{2.17}$$

Where N_z^* is an equivalent-statistically-independent number of zero crossings and defined as

$$N_z^* = \begin{cases} \max(2.1, N_z) & 0.00 < \delta \le 0.10 \\ \left(1.63\delta^{0.45} - 0.38\right) \cdot N_z & 0.10 < \delta \le 0.69 \\ N_z & 0.69 < \delta \le 1.00 \end{cases} \tag{2.18}$$

and δ is a measure of bandwidth defined by Equation (2.14).

[1] http://en.wikipedia.org/wiki/Expected_value#Formulas_for_special_cases
[2] http://stats.stackexchange.com/a/13377/48461

2.2.1.5 Toro and McGuire [1987]

Toro and McGuire [1987] (abbreviated as TM87) adopted the functional form of Equation (2.11) proposed by Davenport [1964] with two modifications. The first modification introduced the non-stationarity factor (n_f)—discussed in Section 3.2—to address the fact that the oscillator does not reach steady-state conditions during the interval [0, T_{gm}]. The second modification addressed the correlation in peaks ignored by the Poisson process assumption and is based on equivalent-statistically-independent number of zero crossings [Der Kiureghian 1980]:

$$N_z^* = \max\left[1.33, \left(1.63\delta^{0.45} - 0.38 \cdot N_z\right)\right] \tag{2.19}$$

The PF is defined as:

$$\text{PF} = \frac{x_{\max}}{x_{rms}} = n_f \left[\sqrt{2\ln\left(N_z^*\right)} + \frac{0.5772}{\sqrt{2\ln\left(N_z^*\right)}}\right] \tag{2.20}$$

2.3 DISCUSSION

To illustrate the differences in the PF formulations, three different events were considered: moment magnitude **M** 3.5 at 5 km, **M** 5.5 at 20 km, and **M** 7.5 at 100 km. Using a point-source source model and Central and Eastern North America (CENA) parameters from Campbell [2003], the associated FAS were computed and are shown in Figure 2.1; SDOF transfer functions with an oscillator natural frequency (f_n) of 0.1, 3.0, and 100 Hz and a damping of 5% were applied to the FAS. The resulting FAS for the three events are shown in Figures 2.2, 2.3, and 2.4. Considering the range of oscillator frequencies, the bandwidth parameters ε and δ are computed using Equations (2.10) and (2.14), respectively. The variation of ε and δ with oscillator frequency is shown in Figures 2.5 and 2.6, respectively. Narrow-band motions were characterized by ε values close to 1 or δ values close to 0.

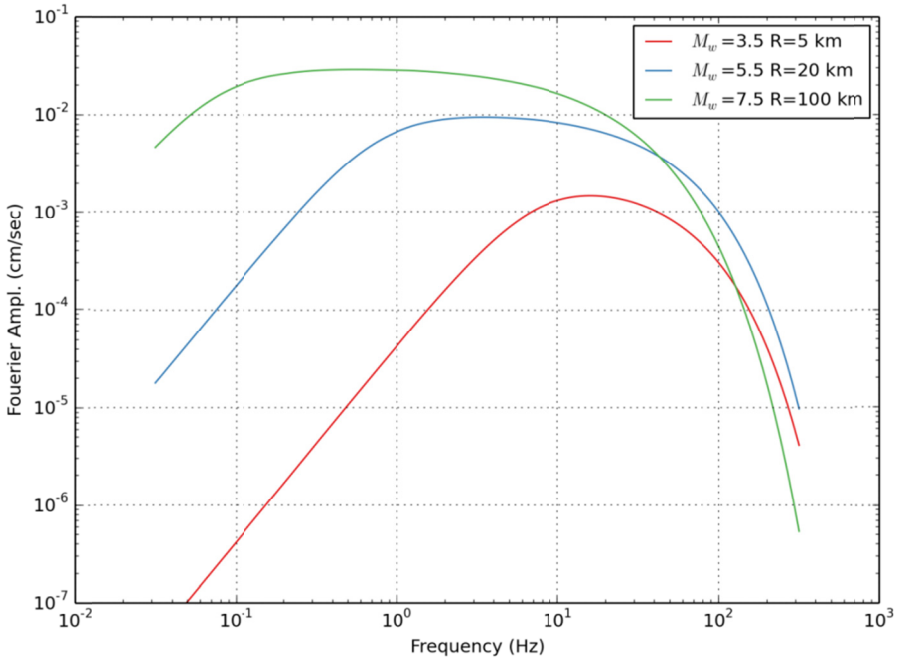

Figure 2.1 **The FAS for the M 3.5 event at a distance of 5 km. The FAS with the SDOF transfer function with f_n of 0.1, 3.0, and 100 Hz and 5% damping are also shown.**

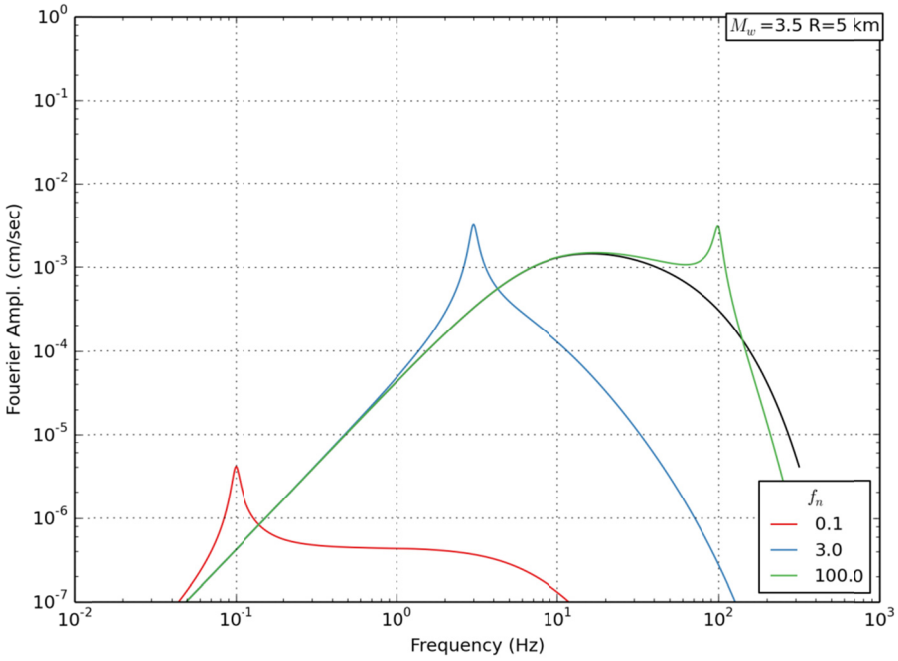

Figure 2.2 **The FAS for the M 3.5 event at a distance of 5 km. The FAS with the SDOF transfer function with f_n of 0.1, 3.0, and 100 Hz and 5% damping are also shown.**

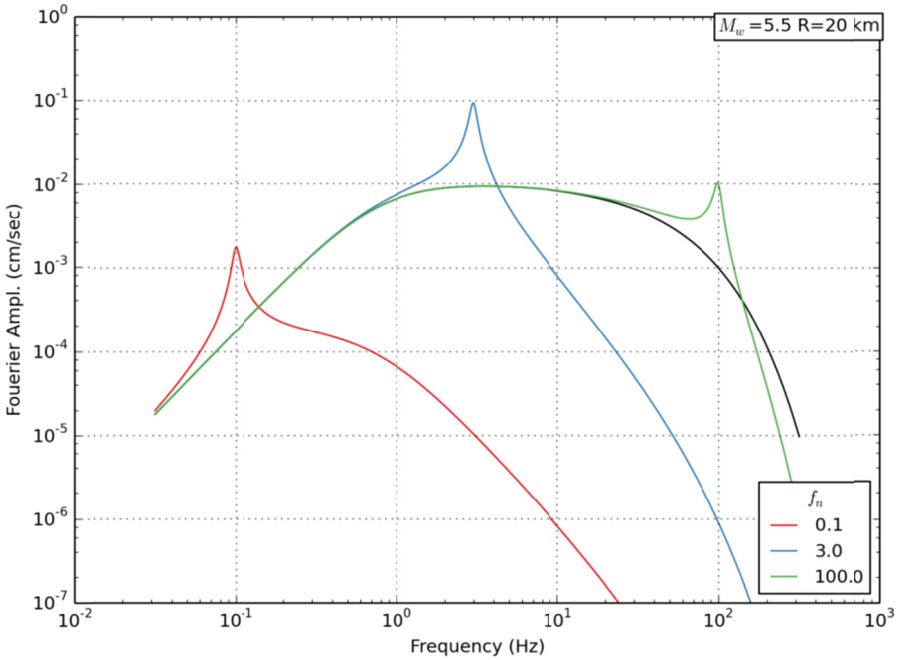

Figure 2.3 **The FAS for the M 5.5 event at a distance of 20 km. The FAS with the SDOF transfer function with f_n of 0.1, 3.0, and 100 Hz and 5% damping are also shown.**

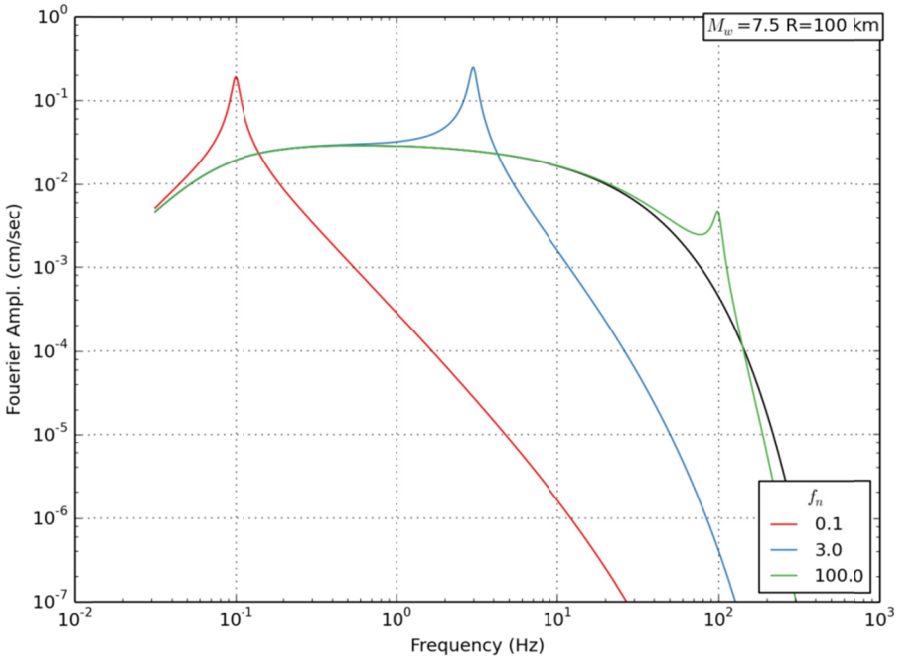

Figure 2.4 **The FAS for the M 7.5 event at a distance of 100 km. The FAS with the SDOF transfer function with f_n of 0.1, 3.0, and 100 Hz and 5% damping are also shown.**

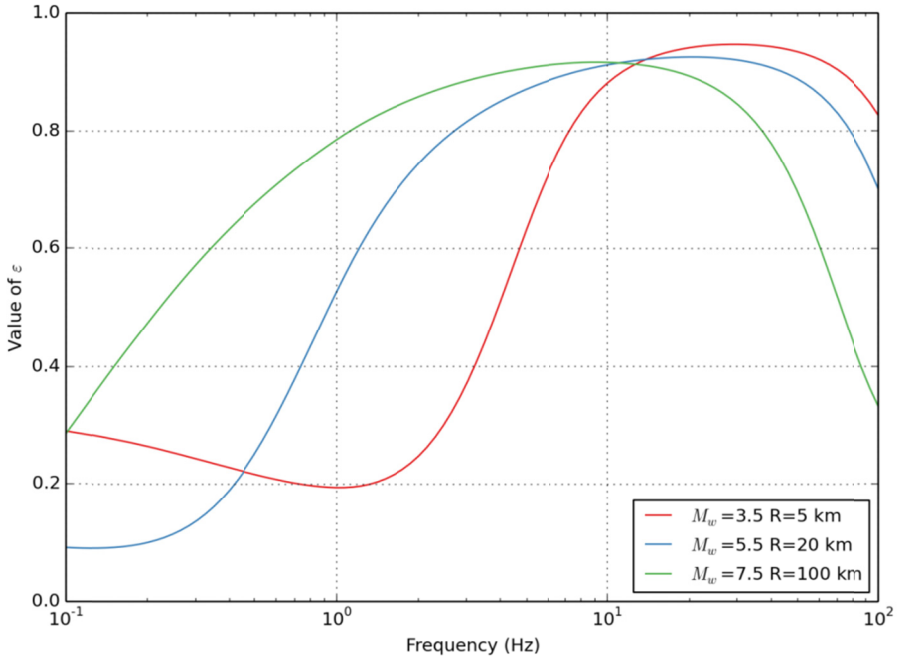

Figure 2.5 **Variation of the bandwidth parameter *ε* with oscillator frequency and the three considered events.**

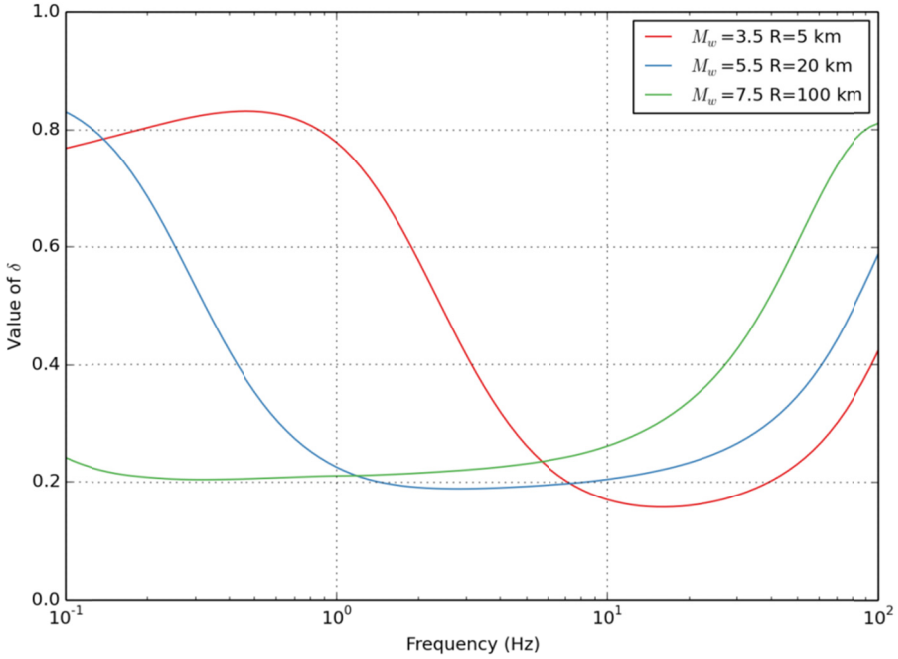

Figure 2.6 **Variation of the bandwidth parameter δ with oscillator frequency and the three considered events.**

The PF formulations presented in the previous section can be separated into two categories: (1) those based on Cartwright and Longuet-Higgins [1956]; and (2) those based on Vanmarcke [1975]. The Cartwright and Longuet-Higgins [1956] formulation factor assumes statistical independence between the local peaks of a random process, which is a significant approximation for a narrow-band process [Der Kiureghian 1980].

To illustrate the differences between the PF formulations, the PFs were computed for the three scenarios using four different PF formulations: CLH56, D64, V75, and DK85. For these calculations, the N_z was limited to be greater than 1.33. The computed PFs are shown in Figures 2.7, 2.8, and 2.9. The differences between each of the formulations vary with respect to input motion and oscillator frequency. For the **M** 5.5 and 7.5 events (Figures 2.8 and 2.9), the considered PFs are clustered with the CLH56 and D64, and demonstrate relatively consistent behavior. Similarly, the V75 and DK85 provide similar estimates of the PF. These results are not unexpected as the two groups of PFs are based on differing assumptions. For the **M** 3.5 event (Figure 2.7), there are significant differences between the CLH56 and D64 due to the limited range over which the asymptotic approximation is accurate. The limit of $N_z \geq 1.33$ also limits the DK85 PF to be greater than 1.51 for frequencies less than 10 Hz.

The differences between the CLH56 and D64, and V75 and DK85 PF formulations suggest that both PF formulations should be considered. While the CLH56 is based on a simpler statistically model (i.e., Poisson process), this methodology is used by SMSIM [Boore 2003], which has been used extensively within the seismology community. The deficiency of assumed statistical independence was addressed first by Boore and Joyner [1984] and has been revisited by subsequent work through modifications of the duration; see Chapter 3. Although the recommended modifications to the ground motion improve the agreement between time series and RVT response spectra, they fail to address the underlying statistical assumptions. These assumptions may lead to inaccurate results with RVT when it is extended beyond calculation of response spectra. Kottke and Rathje [2013] compared time series and RVT seismic site response analyses, and showed significant differences between the results, which in part was due to differences in duration. Ongoing work by Rathje [*Personal Communication* 2014] has shown that using the Vanmarcke [1975] PF formulation reduces these differences.

Both the Cartwright and Longuet-Higgins [1956] and Vanmarcke [1975] PF formulations are recommended for use by this project. The complete form of the Vanmarcke [1975] formulation is recommended because asymptotic formulations, such as Der Kiureghian [1980], are not accurate over the range of bandwidths considered by this project.

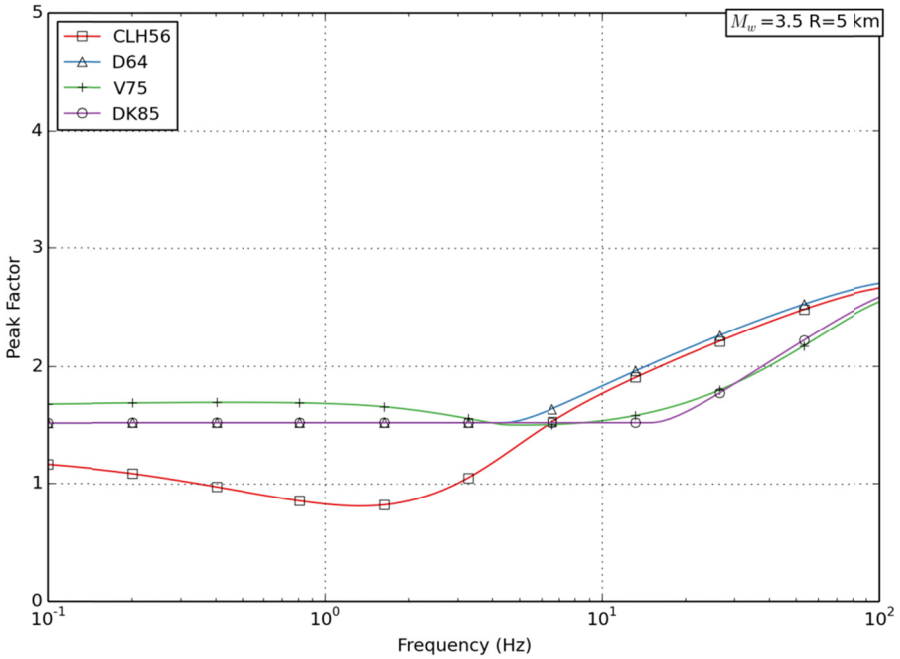

Figure 2.7 **The PFs computed by four different PF formulations at various oscillator frequencies for the M 3.5 event at a distance of 5 km.**

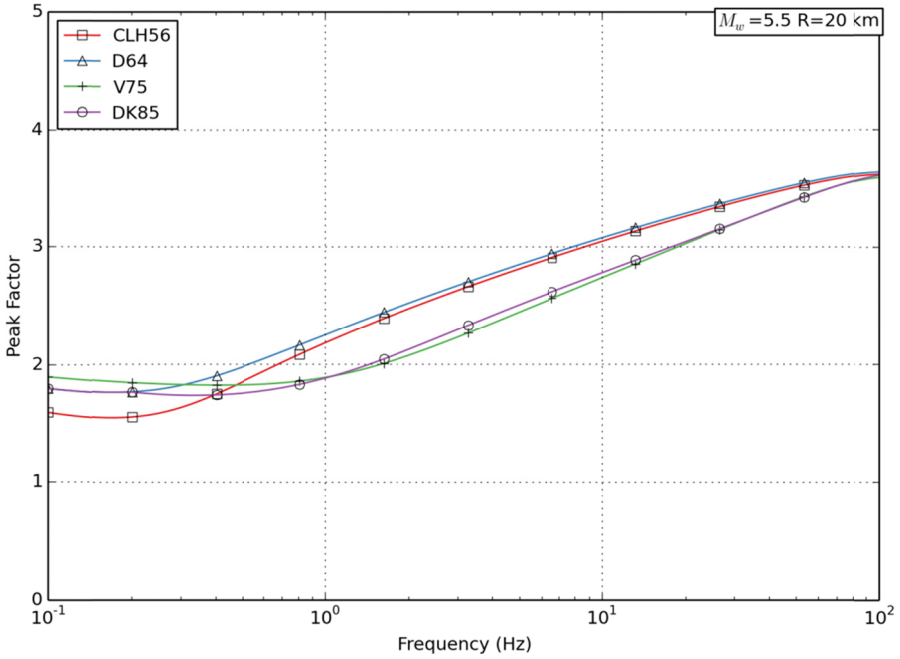

Figure 2.8 **The PFs computed by four different PF formulations at various oscillator frequencies for the M 5.5 event at a distance of 20 km.**

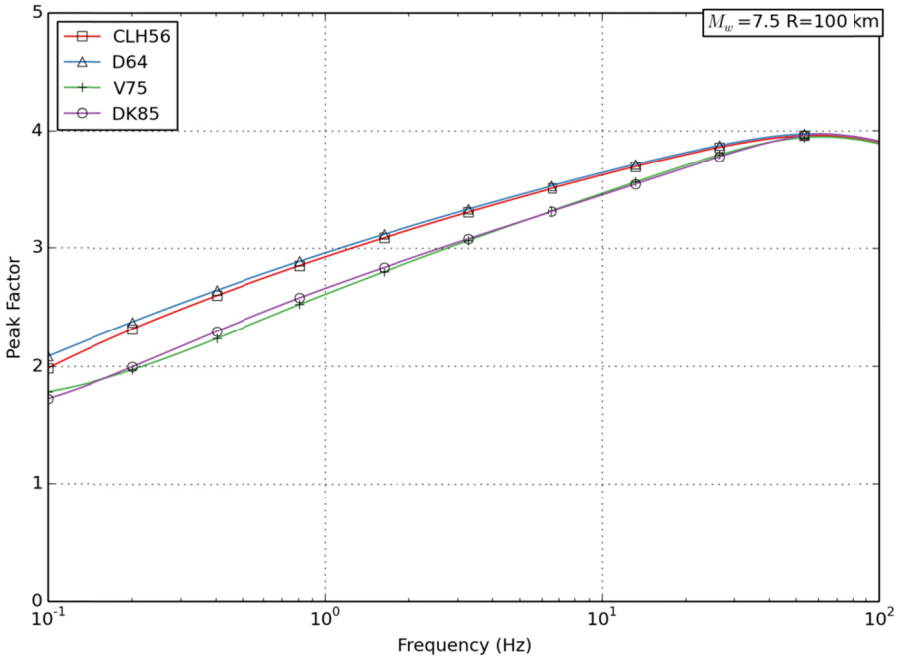

Figure 2.9 **The PFs computed by four different PF formulations at various oscillator frequencies for the M 7.5 event at a distance of 100 km.**

2.4 GROUND-MOTION DURATION

In the context of ground motions, "duration" is the term used to refer to different definitions of time-length intervals. Whenever discussing ground-motion duration, it is important to understand the specific definition of the metric. In some cases, duration can refer to the actual physical duration of ground motions based on threshold or rules; in other cases, as it is for some RVT applications, it can be a fitted parameter with units of time, but it doesn't relate to the traditional concept of shaking duration.

2.4.1 Earthquake Source and Path Durations

Ground-motion duration has long been recognized to be inversely related to the earthquake's corner frequency [Hanks and McGuire 1981]. Herrmann [1985] showed that ground-motion duration also increases with distance. Traditionally, the total ground-motion duration (D_T) is decomposed into two contributing factors: the source duration (D_S) and the path duration (D_P). The source duration for a single-corner frequency model is given by:

$$D_S = 1/f_c \tag{2.21}$$

where f_c is the corner frequency [Hanks and McGuire 1981; Herrmann 1985; and Boore 2003]. The double-corner frequency model is often given as:

$$D_S = 1/f_a \tag{2.22}$$

where f_a is the lower of the two corner frequencies (e.g., Atkinson and Boore [1995] and Atkinson and Silva [2000]). Boore et al. [2014], however, have suggested that the duration should be modeled as a combination of the two corner frequencies, i.e.,

$$D_S = \frac{0.5}{f_a} + \frac{0.5}{f_b} \tag{2.23}$$

As formulated by Hanks and McGuire [1981] and Boore [1983], the ground-motion duration only included D_S. Thus, for a given magnitude, D_T was the same at all distances. Herrmann [1985] noted that this formulation should be limited to short distances because the duration of real ground motions increases with distance. Herrmann [1985] computed synthetic records with a one-dimensional velocity model to illustrate this trend, noting that the ground motion at short distances is simple and pulse-like, while at larger distances surface waves and crustal reflections arrive after the direct *S*-wave, increasing the duration of shaking. Herrmann [1985] proposed that the path duration could be modeled as:

$$D_P = 0.05R \tag{2.24}$$

where R is the hypocentral distance.

For an assumed source model, the D_P can be computed empirically by subtracting the D_S from D_T, which is typically a function of distance (e.g., Boore [2003]). As discussed below, there are different ways to compute D_T from ground-motion records. The following subsections discuss the different parameterizations of D_T as well as recently developed models for D_P.

2.4.2 Significant Durations

For many ground-motion applications, the significant duration, bracketed duration, and uniform duration are often used to characterize the duration of ground-motion shaking. Herein, only the significant duration as introduced by Trifunac and Brady [1975] will be discussed. It is based on the normalized integral of the squared acceleration (i.e., the Husid curve) and is closely associated with the "rms" acceleration.

The Arias intensity at time $t[I_a(t)]$ is computed by:

$$I_a(t) = \frac{\pi}{2g}\int_0^t x(t)^2\,dt \tag{2.25}$$

where $x(t)$ is the acceleration at time t in units of gravity (g). The Husid curve $[h(t)]$ is defined as:

$$h(t) = \frac{I_a(t)}{I_a(\infty)} \tag{2.26}$$

and varies from zero at the start of a record to one at the end of a record. The significant duration D is defined as the difference in the times at which $h(t)$ for two different percentages of its final

value (Figure 2.10). For example, $D_{5\text{-}95}$ refers to the time difference of the 5–95% occurrence of the squared acceleration.

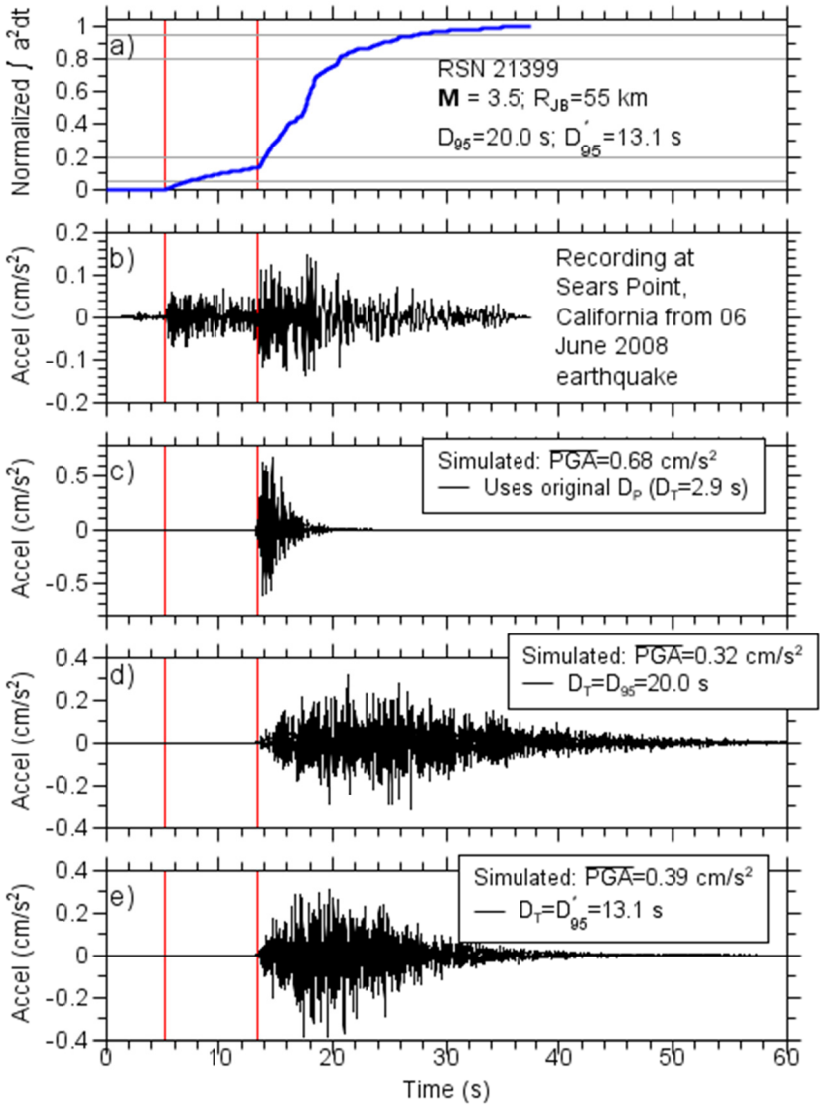

Figure 2.10 **The Husid plot (graph a) from the acceleration record shown in graph (b). For this record, the 0.05 level is reached near the *P*-wave arrival. Graphs (c), (d), and (e) show simulations using D_T values equal to the original path duration and the $D_{5\text{-}95}$ and $D'_{5\text{-}95}$ durations obtained for the recording, respectively. Note the change of the ordinate scale of part (c) compared to the other two simulations. The time series shown for each duration model is the one simulation out of 800 that had a PGA closest to $\overline{\text{PGA}}$. The vertical lines indicate the *P*- and *S*-wave arrivals (the simulations have been aligned on the *S*-wave arrival).**

Alternative measures of duration are based on fitting ground-motion IMs calculated from the recorded motions and predicted by RVT. The IMs used in these parameterizations of duration include the PGA [Vanmarcke and Lai 1980], PGV [Atkinson 1993b; 1995], and PSA at a

number of periods [Bora et al. 2014]. This last definition of duration could be interpreted as the most relevant for RVT applications and is discussed in Section 2.3.3.

The stochastic method of ground-motion simulation, as developed by Boore [1983], used $D_{5–95}$ as the total duration of ground shaking and a separate duration to compute peak values (i.e., spectral accelerations), which is a function of the oscillator period. Thus, significant duration may still be preferred as the parameterization for ground-motion duration for use within the Boore [1983] framework for a number of reasons: (1) the duration of ground-motion excitation is conceptually distinct from the duration of a responding oscillator (as in Boore and Thompson [2012, 2015]); (2) it provides consistency and continuity with the Boore formulation [1983; 2003]; (3) the widespread use and availability of $D_{5–95}$; and (4) the ambiguity as to which IM to use for IM-compatible durations.

2.4.2.1 Ou and Hermann [1990]

A fundamental assumption underlying RVT is that the signal is stationary; see Section 2.3.3. Given that, Ou and Herrmann [1990] argued that the duration window should be chosen such that a stationary process can approximate the signal. Their criteria for determining that a time window is near-stationary is that the Husid plot increases approximately linearly throughout that time window. They analyzed records from the Eastern Canada Telemetered Network with epicentral distances ranging from 135–994 km and concluded that the $D_{5–75}$ window is approximately stationary. They validate the use of this window with RVT by comparing the measured peaks to the peaks predicted by RVT, noting that the spectrum should be estimated only from the signal within the $D_{5–75}$ time window when D_{75} durations are used in the RVT calculations.

2.4.2.2 Boore and Thompson [2014]

Boore and Thompson [2014] addressed the non-stationarity of ground motions using a different approach. This approach was developed by Boore and Joyner [1984] whereby the duration of the ground motion is treated independently from the non-stationarity correction. A different duration (termed D_{rms} and discussed in detail later) is used to compute the peak values from the "rms" acceleration, which is a function of oscillator period and accounts for the non-stationarity of the signal. Thus, Boore and Thompson [2014] developed a new parameterization of duration that was guided by two primary factors: (1) the use of $D_{5–95}$ was preferred for consistency's sake, in particular for defining the Saragoni and Hart [1974] exponential shaping window in the time domain; and (2) the influence of strong *P*-wave energy and late-arriving surface wave energy should be minimized because the stochastic method is founded upon seismological consideration of *S*-waves.

The problem of early *P*-wave energy is illustrated in Figure 2.10. The Husid plot of the recording is given in the top panel, and the record (second to the top panel) is compared to stochastic simulations where all parameters are held constant except for D_T. The arrival times of the *P*- and *S*-waves are labeled on each plot, and the simulations are aligned to coincide with the *S*-wave arrival. The D_T and the median PGA from 800 simulations ($\overline{\text{PGA}}$) are given for each simulation.

The main purpose of Figure 2.10 is to demonstrate that the 5% level for data is reached substantially earlier than the *S*-wave arrival in some cases. That said, parts (c), (d), and (e) of the figure also demonstrate the consequences of the different durations for simulated ground motions. Figure 2.10(c) shows that the $D_P = 0.05R$ duration is too short, whereas Figure 2.10(d) shows that using D_{5-95} from the recorded time series overestimates the path duration because of the presence of strong *P*-wave energy. Figure 2.10(e) shows the duration parameter developed by Boore and Thompson [2014] (defined below as D'_{95}). Note that the simulations can be compared in terms of the total duration but also in terms of their respective $\overline{\text{PGA}}$: the larger the D_T, the smaller the amplitude (by approximately the inverse of the square root of D_T) because the energy is spread across a larger time window. The median PGA (indicated by $\overline{\text{PGA}}$) for the 800 simulations is given in the legends; as expected, the ratios of any two simulations are close to the square-root of the ratio of their durations.

The early start to the duration measure illustrated in Figure 2.10 is incompatible with the assumption that simulations are for the *S*-wave contribution to the ground motion. Similar problems can occur due to a delay of the time at which the 95% level is reached. These effects imply that the shape of the envelope of ground motion from data may be inconsistent with that assumed in the simulations. To avoid the instability due to the early and late times at which the 5% and 95% levels are reached, respectively, Boore and Thompson [2014] proposed an effective duration D'_{5-95}:

$$D'_{5-95} = 2.0(D_{80} - D_{20}) \tag{2.27}$$

The scale factor of 2.0 is based on the average of the ratio of D_{5-95} to $(D_{80} - D_{20})$ from the simulations.

Boore and Thompson [2014] computed path durations from the NGA-West1 (for active crustal regions [ACRs]) database as $D_P = D'_{95} - D_S$, and fit a piecewise linear function to the data. Boore and Thompson [2015] performed a similar analysis of the NGA-East database (for stable continental regions [SCRs]). The difference in D_p for ACRs and SCRs is shown in Figure 2.11, which plots D_p as a function of distance R_{PS} (which is the adjusted point-source distance to account for finite-fault effects). Figure 2.11 shows the Boore and Thompson [2015] function and median values for SCRs and the Boore and Thompson [2014] function and median data values for ACRs; path durations for individual records for SCR **M** 4–5 data are included to illustrate the scatter in the data. In addition, the path duration used in a number of simulations of Eastern North America (ENA) ground motions (e.g., Atkinson and Boore, [1995; 2006]) is also shown. The longer durations for SCRs compared to ACRs might be the result of the smaller intrinsic attenuation in the cooler crust, which allows the scattered waves to prolong the duration of shaking.

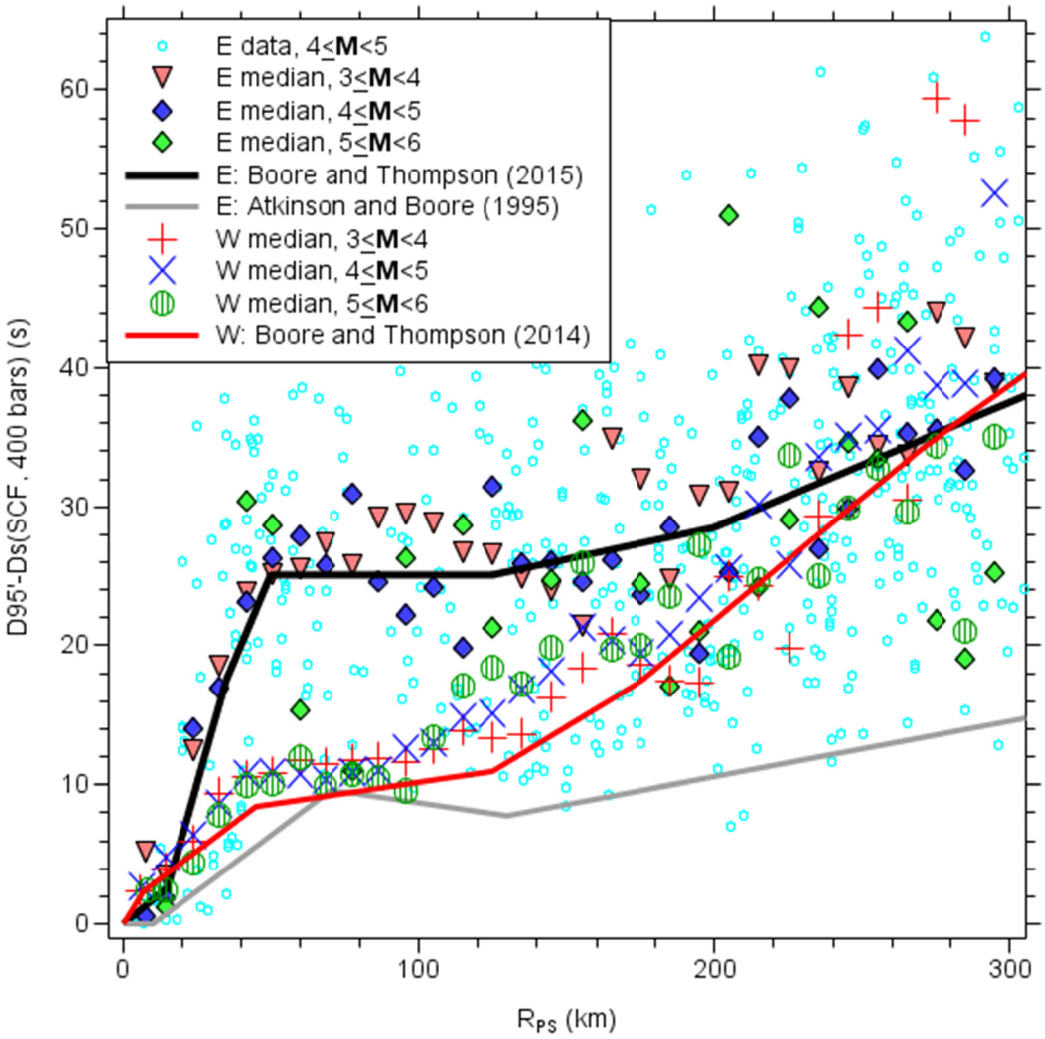

Figure 2.11 **The medians in various magnitude and distance bins of $D_P = D'_{95} - D_S$ for data from both from eastern North America ("E") and active crustal regions ("W"). Path durations computed from individual records for M 4–5 are included to illustrate the scatter in the data. For comparison, D_P functions are included from Boore and Thompson [2014; 2015] and Atkinson and Boore [1995].**

2.5 DURATIONS FOR RESPONSE SPECTRUM COMPATIBLE GROUND MOTIONS

An important ingredient in the RVT framework is the duration of ground motion [Hanks and McGuire 1981; Vanmarcke and Lai 1980; and Boore, 1983, 2003]. It enters into calculation of the maximum response:

$$x_{\max} = p_f \cdot y_{\text{rms}} \tag{2.28}$$

both in the PF, p_f, and in the "rms" motion, y_{rms}. Traditionally, different measures of duration based on different criteria (e.g., cumulative energy and bracketed) have been proposed. Based on the application, a suitable duration is selected; however, for RVT it is not entirely clear which duration measure should be used in calculation of response spectra.

Recently, Bora et al. [2014] proposed a duration that is rooted in the RVT framework. It is different from other duration measures: (1) it is not based on an acceleration time series; and (2) it is not a "duration" in a physical sense but a parameter suitable to calculate response spectra using RVT. The duration proposed in Bora et al. [2014] is defined as the duration that minimizes the misfit between the observed response spectrum and the one calculated from the observed FAS and RVT. Thus, in an application that aims to predict response spectra, this duration measure is ideally suited for the RVT framework. Basically, the duration is treated as a parameter that is inverted for using RVT as the model and the response spectrum and the FAS as data. Therefore, one should refrain from associating any physical meaning with this duration: it is to be used as a parameter within RVT to predict response spectra together with the empirical FAS. The advantage of treating the duration as a parameter is that it absorbs any mis-specification of the model.

Equation (2.28) shows the relation between the "rms" duration and the maximum oscillator response. If Davenport's [1964] PF is used, the relation becomes:

$$x_{\max} = \left(\sqrt{1 \ln N_z} + \frac{0.577}{\sqrt{2 \ln N_z}} \right) \cdot \sqrt{\frac{m_0}{D_{\text{rms}}}} \tag{2.29}$$

with N_z the expected number of zero crossings, and m_k the kth spectral moment: see Section 2.2.1. Because the spectral moments can be calculated from the FAS [i.e., $X(f)$], Equation (2.29) contains only one unknown parameter: the duration D_{rms}. Hence, D_{rms} can be inverted by minimizing the misfit (ξ) between the observed response acceleration spectrum [$S_a(f)$] and the RVT-calculated maximum response $[x_{\max}(f)]$. Since the response spectrum is log-normally distributed, the misfit is calculated as:

$$\xi = \sum_f [\ln S_a(f) - \ln x_{\max}(f)]^2 \tag{2.30}$$

Note: although the idea of an optimized duration is independent of the specific PF formulation, it is important to be consistent. For each PF formulation, an optimized duration can be estimated, but because these two are tied together, forward calculations need to be made with the same assumptions/formulations that were used in the inversion of the duration.

As an example, durations were calculated for two records using both the PF of Cartwright and Longuet-Higgins [1956] and that of Davenport [1964]. One of the records is from the Saguenay event with an epicentral distance of 442 km (record ID 70 in the NGA-East database). The other record is from the Mineral event (record ID 8365 in the NGA-East database). Table 2.1 presents the calculated durations. Figure 2.12 shows the corresponding observed response spectra and the RVT-calculated spectra. The durations based on the different PF formulations vary, but the misfit is close in both cases, and the RVT-calculated response spectra are very

similar. Hence, if the calculations are internally consistent—forward calculations are done with the same PF as the inversion for the duration—the results are close.

Up to this point in the inversion it has been assumed that D_{rms} and the actual ground-motion duration are the same. In application of the stochastic method, an adjustment is needed to match (1) response spectra calculated via RVT and (2) those based on time-domain simulations [Boore and Joyner 1984; Liu and Pezeshk 1999; and Boore and Thompson 2012]. Theoretically, such a model could be incorporated into the inversion process.

When the duration is optimized against response spectra, it is the appropriate duration to use if the goal is to predict response spectra. Therefore, an empirical FAS model as well as a model for the spectrum-compatible duration can be used that predicts the FAS and duration as a function of magnitude, distance, and other source- and site-related parameters. When the predictions are combined via the RVT framework, a response spectrum prediction is obtained. Refer to Bora et al. [2014] for greater detail.

Table 2.1 **Optimized durations D_{rms}, calculated for two different PF formulations: Cartwright and Longuet-Higgins [1956] (CLH56) and Davenport [1964] (D64), and the associated misfit ξ.**

Record	Formulation	D_{rms} (sec)	ξ
ID 70 (Saguenay)	CL56	34.05	4.32
	D64	34.59	4.33
ID 8365 (Mineral)	CL56	47.80	5.81
	D64	48.85	5.84

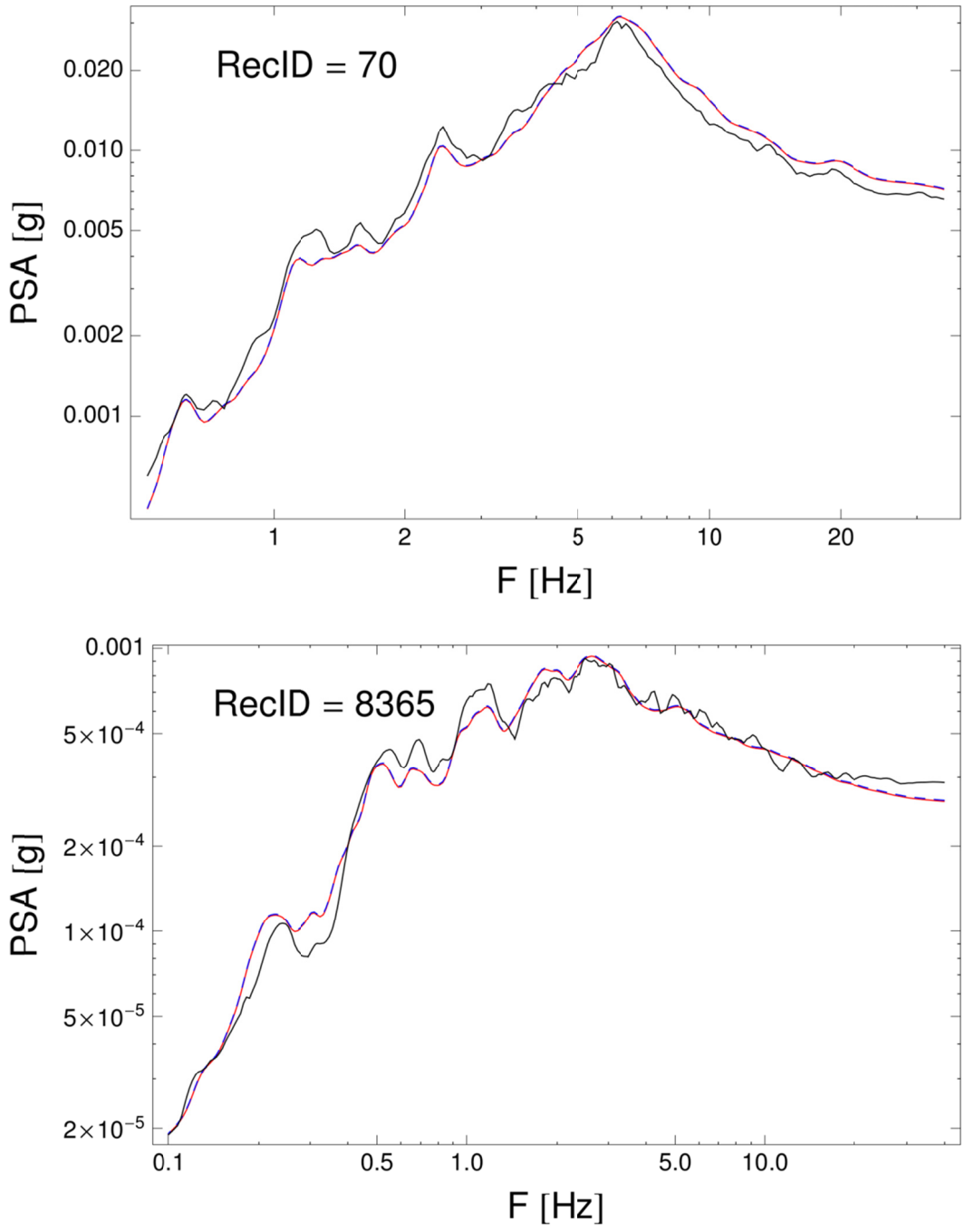

Figure 2.12 **Comparison of response spectrum calculated from the time domain (black) and response spectrum calculated via RVT, with the duration inverted using the PF of Cartwright and Longuet-Higgins (blue) and that of Davenport (red). Top: Record ID 70, Saguenay event. Bottom: Record ID 8365 from the Mineral event.**

3 Corrections for Non-Stationarity

Ou and Herrmann [1990] demonstrated that for peak values such as PGA and PGV, the careful selection of a window can overcome much of the non-stationarity problem. But for resonant systems, such as SDOF oscillators or layered soils, the problem of non-stationarity is an issue. For these systems, there are two methods for adjusting the PFs to correct for non-stationarity:

- modifying the duration of the motion
- directly scaling the PF

This section presents methods developed to address the non-stationarity of response spectra independent of the ground-motion duration.

3.1 NON-STATIONARITY CORRECTIONS BASED ON DURATION MODIFICATION

3.1.1 Boore and Joyner [1984]

Boore and Joyner [1984] explicitly separated the duration used for computing the number of zero crossings and extrema from the duration used to compute the "rms" acceleration of the ground-motion intensity measure (GMIM). The number of zero crossings and extrema are computed from the characteristic frequency (a function of the spectral moments) and the duration of shaking, which is assumed to be D_T (sometimes termed D_{EX} for the duration of excitation). D_T is inappropriate for computing the "rms" response from the amplitude spectrum of the oscillator because it will continue to respond after the ground motion has stopped. This is illustrated in Figure 3.1 (Figure 19 in Boore [2003]), which shows the response of a 10-sec oscillator to a small (**M** 4) and large (**M** 7) earthquake. Boore and Joyner [1984] found that the following equation captured the interaction between the oscillator's duration and the ground-motion duration:

$$D_{\text{rms}} = D_T + D_0 \left(\frac{\gamma^n}{\gamma^n + \alpha} \right) \tag{3.1}$$

where $\gamma = D_T / T_0$; T_0 is the period of the oscillator, $D_0 = T_0/(2\pi\zeta)$ is the oscillator duration, and ζ is the fractional damping of the oscillator. Boore and Joyner [1984] selected constants n and α by comparing different values to data and set them to 3 and 1/3, respectively.

3.1.2 Liu and Pezeshk [1999]

Liu and Pezeshk [1999] developed an improved relationship for D_{rms} in which the value of α in Equation (3.1) is replaced by k, which is a parameter calculated from the ground motion by:

$$k = \sqrt{2\pi\left(1 - \frac{(m_1)^2}{m_0 \cdot m_2}\right)} \tag{3.2}$$

where m_i are spectral moments (*zero*[th], first, and second are considered here) as defined by Equation (2.4). With this substitution, they also found that a better value for n is 2.

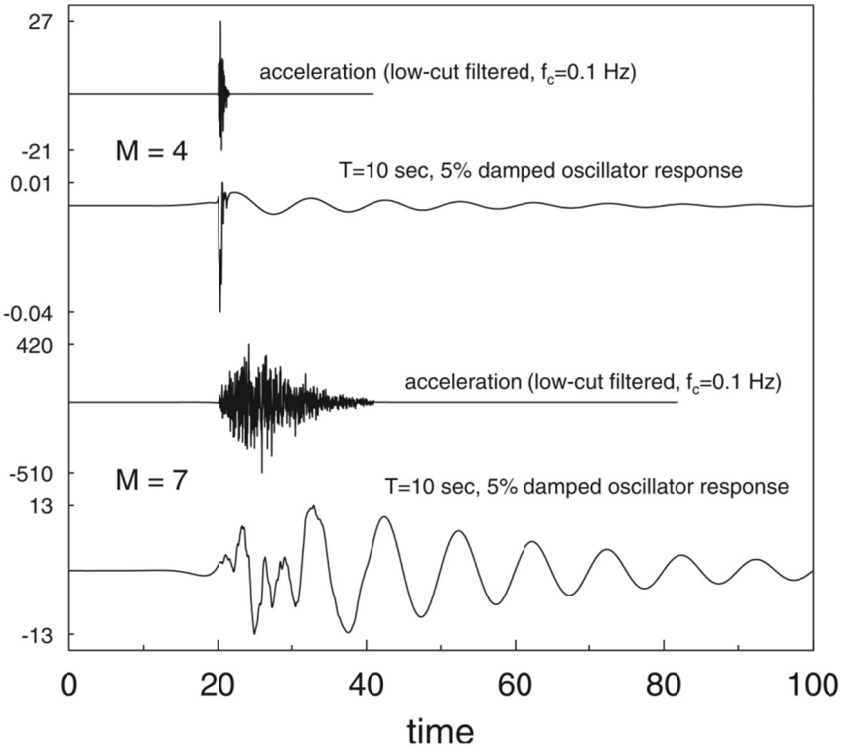

Figure 3.1 **Simulated acceleration time series and computed response of 10.0-sec, 5%-damped oscillator for M 4 and M 7 earthquakes at a distance of 10 km. Because the relative shape is important, each trace has been scaled individually (the actual amplitudes are given to the left of the *y*-axis—acceleration in cm/sec^2 and oscillator response in cm) (reproduced from Boore [2003]).**

3.1.3 Boore and Thompson [2012]

Boore and Thompson [2012] noted that after using the modifications discussed above, clear trends in the GMIM residuals still existed, particularly for small-to-moderate magnitudes and moderate-to-large distances. Therefore, they generalized the D_{rms} equation to be able to model more variations of D_{rms} with magnitude, distance, and period. They noted that D_{rms} can be solved in terms of the time-domain peak values (y_{td}) and the RVT peak values with no oscillator correction (y_{xo}; i.e., $D_{\text{rms}} = D_T$)

$$D_{\text{rms}} = D_T (y_{xo} / y_{td})^2 \tag{3.3}$$

This equation can be rearranged so that ratio of the durations is equal to the squared ratio of the peaks

$$D_{\text{rms}} / D_T = (y_{xo} / y_{td})^2 \tag{3.4}$$

Figure 3.2 plots the squared peak ratios against period and against period normalized by the ground-motion duration for a range of magnitudes and distances; see Boore and Thompson [2012] for the parameters of the stochastic model used to generate these curves. This figure illustrates the effect of normalizing the period by the ground-motion duration where much of the apparent variability in D_{rms} / D_T is reduced. For this reason, Boore and Thompson [2012] modified the general function form for D_{rms} used by Boore and Joyner [1984] and Liu and Pezeshk [1999] to be

$$\frac{D_{\text{rms}}}{D_T} = 1 + \frac{1}{2\pi\zeta}\left[\eta / (1 + \alpha\eta^n)\right]$$

where $\eta = T_0 / D_T$. Additional terms were then added to better fit the observed ratios:

$$\frac{D_{\text{rms}}}{D_T} = \left(c_1 + c_2 \frac{1 - \eta^{c_3}}{1 + \eta^{c_3}}\right)\left[1 + \frac{c_4}{2\pi\zeta}\left(\frac{\eta}{(1 + c_5\eta^{c_6})}\right)^{c_7}\right] \tag{3.5}$$

In this function, α and n are now free coefficients (c_5 and c_6) to be estimated from the data, and the function approaches $c_1 + c_2$ as η approaches zero and $c_1 - c_2$ as η approaches infinity. Boore and Thompson [2012] fit the coefficients of this equation to the squared ratios $(y_{xo} / y_{td})^2$, where the coefficients vary with magnitude and distance. They developed one set of coefficients from a seismological model that is appropriate for use in SCRs and one that is appropriate for ACRs. Inspection of the squared ratios from these two different sets of simulations clearly indicates that the D_{rms} correction depends upon the seismological model. Additionally, there have been a number of updates to the stochastic method published since Boore and Thompson [2012]; thus the coefficients needed to be updated, as discussed next.

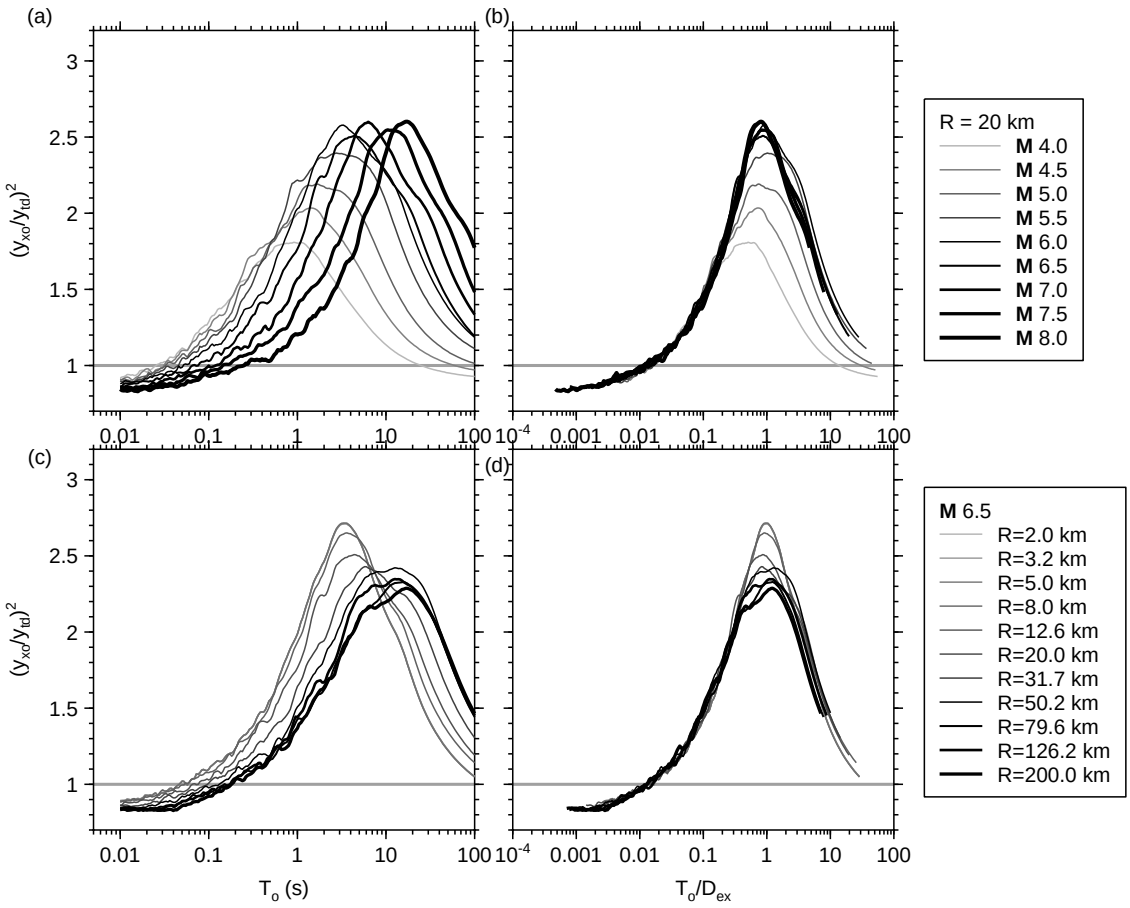

Figure 3.2 **Squared ratios of PSA from random-vibration simulations (for which $D_{rms} = D_T$; i.e., no oscillator correction) and time-domain simulations. Note that D_{EX} is synonymous with D_T; see Boore and Thompson [2012] for details of the stochastic model. Left panels: the squared ratios are plotted against period (T_0). Right panels: the squared ratios are plotted against T_0 normalized by the ground motion duration (T_0/D_T). The top row shows ratios for a fixed distance (20 km) and a suite of magnitudes; the bottom row shows ratios for a fixed magnitude (6.5) and a suite of distances.**

3.1.4 Boore and Thompson [2014; 2015] and Update to Boore and Thompson [2012]

Subsequent to Boore and Thompson [2012], a number of important updates have been made to the stochastic method that will affect D_{rms}/D_T. These include:

- Revised path durations [Boore and Thompson 2014; 2015]
- Revised crustal amplifications [Boore and Thompson 2015]
- Generalized double-corner frequency source model [Boore et al. 2014]
- Adjustments to the finite-fault correction factor [Yenier and Atkinson 2014; Boore et al. 2014]

- A new "rms"-to-PF (R2PF) based on Vanmarcke [1975] and Der Kiureghian [1980]

Figure 3.3 shows spectral displacements for a standard SCR model (equivalent to that used in Atkinson and Boore [2006]) computed using TD and RV computations. The bottom row shows ratios of the RV/TD simulations. Although the RV simulations using the Der Kiureghian [1980] R2PF are closer to the TD simulations (which are taken as the correct values) for small magnitudes and short periods than those using the Cartwright and Longuet-Higgins [1956] R2PF, neither R2PF is acceptably accurate; additional curves were added to Figure 3.3 for the Boore and Thompson [2012] D_{rms} model. While the Boore and Thompson [2012] coefficients work relatively well for the CL R2PFs (which were used in the RV simulations by BT12), they do not work well for the DK R2PFs. Thus, the coefficients need to be recomputed for the new R2PF and seismological parameters for SCRs and ACRs.

To check that the coefficients were estimated accurately, the TD/RV ratios were plotted for a range of magnitudes, distances, and periods. Figure 3.4 shows maps of the ratio TD/RV for a SCR model as a function of period and distance for the range of magnitudes used in the simulations (2 to 8). In these figures, period rather than frequency was used to be consistent with the published sources. The top row shows the ratio TD/RV with no adjustment to D_{rms}. The second row shows the ratio when the RV simulations used the value of D_{rms} from Boore and Thompson [2014], which were derived by fitting the ratios in the top row of the figure (note the expanded scale compared with that of the top row of graphs). This indicates that the D_{rms} correction is sufficiently accurate across the magnitude, distance, and periods of interest.

Next, the consistency of the TD/RV ratios was evaluated as reasonable changes were made to the seismological model. Figure 3.5 shows the TD/RV ratios for SCR models with somewhat different parameters than the base model used in deriving the coefficients for D_{rms}. Note the expanded scale used for the graphs (0.9 to 1.1). All of the SMSIM parameter files used in the simulations for the TD and the RV simulations are given in the electronic supplement of Boore and Thompson [2015]. The first and second rows in Figure 3.5 are for the same model used to derive the coefficients (i.e., the base model) but with stress parameters of 100 bars and 1600 bars, respectively, rather than 400 bars. The results imply that the adjustments to D_{rms} are relatively insensitive to the stress parameter. The models used in the third and fourth rows depart even farther from the base model. The third row uses parameters that are consistent with the Atkinson and Boore [2006] model; the most important differences between this model and the base model are path duration, geometrical spreading, and attenuation functions. The graphs in the fourth row use a double-corner-frequency source model given by Atkinson [1993a], but otherwise the parameters are the same as those in the base model. Except for those events that are of little interest (e.g., very small magnitudes or long periods), the results in Figures 3.4 and 3.5 show that relatively accurate results (within about 10% for the examples discussed herein) can be obtained for RV simulations using D_{rms} values obtained for models that are different than the models for which the simulations are being done.

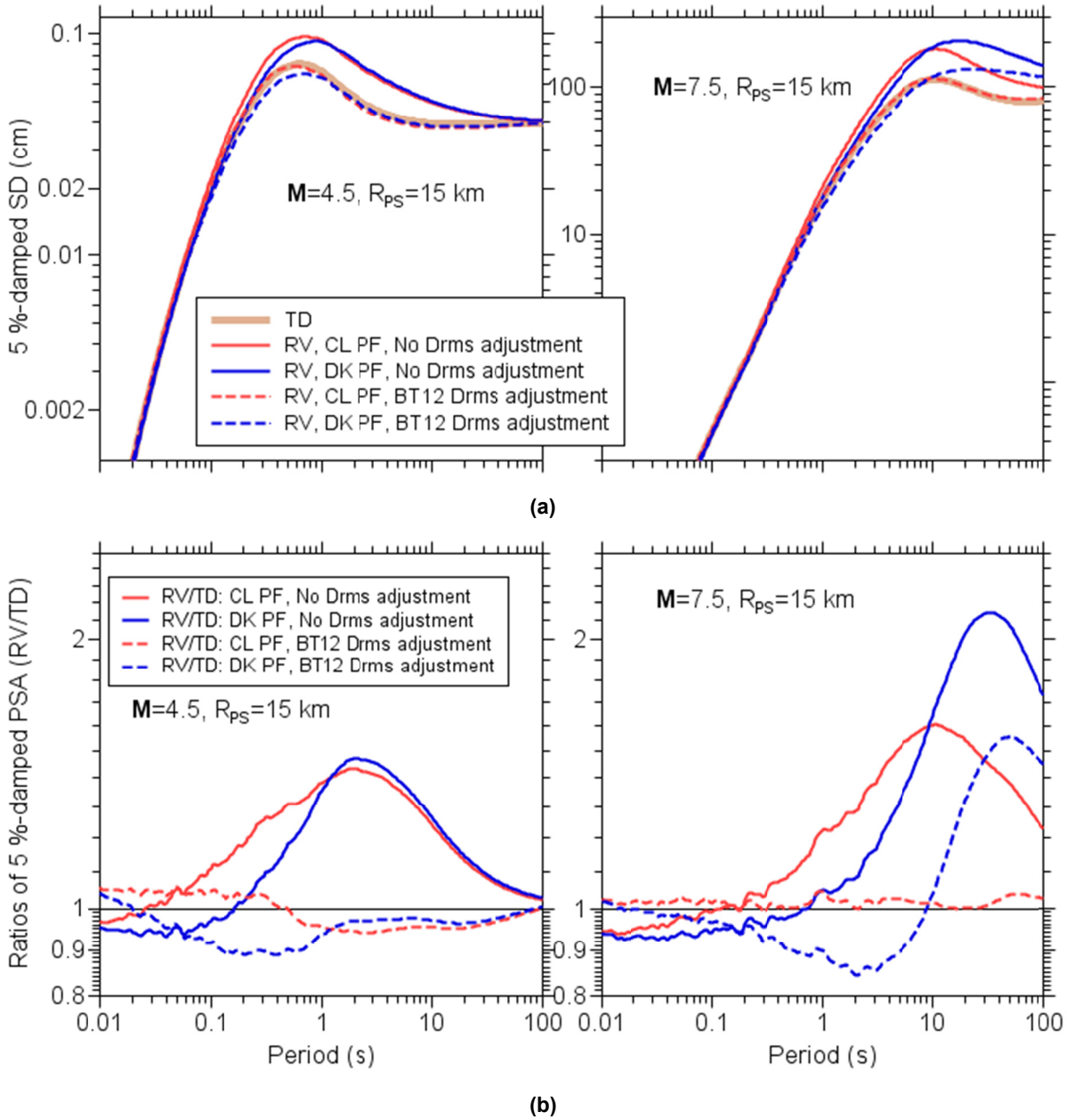

Figure 3.3 **(a) Response spectral displacements (SD) from time-domain (TD) simulations and random-vibration (RV) simulations, with and without adjustments for the duration (D_{rms}) used to compute the "rms" of the oscillator response. For the RV simulations, two "rms"-to-PFs were used: Cartwright and Longuet-Higgins [1956] (CL) and Der Kiureghian [1980] (DK); and (b) ratios of the RV and TD response spectra.**

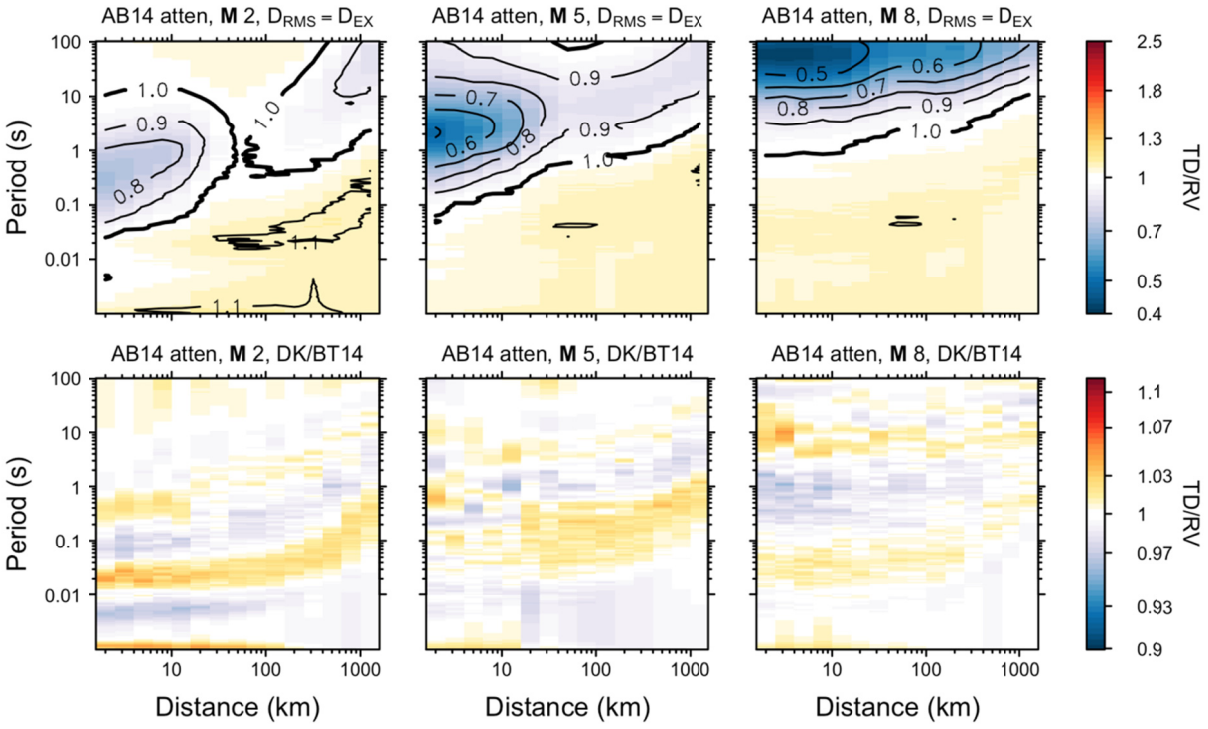

Figure 3.4 **Shaded contour plots of the TD/RV ratios; see Boore and Thompson [2015] for the parameters used to generate the TD and RV simulations. The top row shows the ratios when $D_{rms} = D_T$ in the RV simulations, and the bottom row shows the TD/RV ratio using the new adjustments to D_{rms} given in the electronic supplement of Boore and Thompson [2015]. Note the change of scale between the top and bottom rows.**

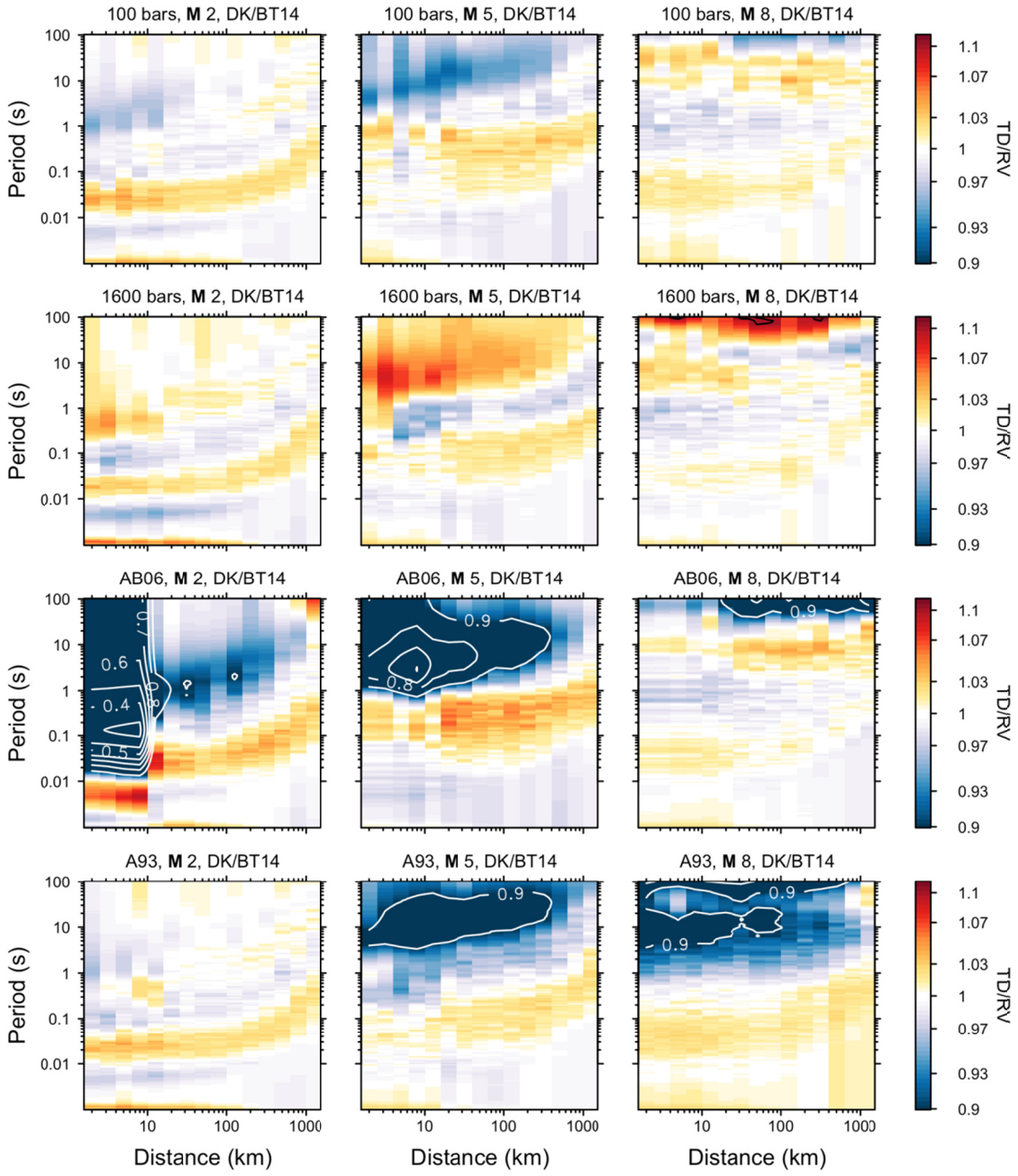

Figure 3.5 **Shaded contour plots of the TD/RV ratios for various SCR models not used to derive the coefficients used in the RVT simulations; see text and Boore and Thompson [2015] for discussion and model details. DK = the Der Kiureghian [1980] R2PF; BT14 = the new coefficients for Equation (5) given in the electronic supplement; AB06 = Atkinson and Boore [2006]; and A93 = Atkinson [1993a].**

3.2 NON-STATIONARITY CORRECTIONS BASED ON PEAK FACTOR MODIFICATION

Section 8.3.2 of Vanmarcke [1976] considered the time-dependent response of a SDOF oscillator. Integrating the transient squared amplification function over all frequencies yields the following scale factor:

$$n_f = \sqrt{1 - \exp(-4 \cdot \pi \cdot \zeta \cdot f_n \cdot T_{\text{gm}}} \tag{3.6}$$

where ζ and f_n are the damping and natural frequency, respectively, of the SDOF transfer function. This non-stationarity factor corrects for the fact that an oscillator may not reach steady-state conditions during the interval from 0 to D_{gm}. The response within the duration of the ground motion $[x_{\text{rms}}(T_{\text{gm}})]$ is related to the steady-state response $[x_{rms}(\infty)]$ by Toro and McGuire [1987]:

$$x_{\text{rms}}(T_{\text{gm}}) = x_{\text{rms}}(\infty) \cdot n_f \tag{3.7}$$

3.3 DISCUSSION AND SUMMARY

This section presents two methods for modifying RVT methodology. The influence of these corrections is evaluated by computing the ratio of the oscillator response computed by the corrected and uncorrected approaches presented in Table 3.1. The TM87 method is not represented here because the same corrective factor is used by the V75 formulation. The ratio between corrected and uncorrected oscillator response for the three events considered in Section 2.2.2 are shown in Figure 3.6. For the BT12 "rms"-duration correction, the coefficients for the CENA region were used. For the **M** 3.5 event, the five different correction methods provide very different estimates. Because the BT12 method only provides coefficients down to **M** 4, the corrective ratio for BT12 is not shown in Figure 3.6. The least significant ratio (i.e., closest to 1), is the DK85 ratio, although based on modifying the N_z parameter to fit empirical results, it does not explicitly consider non-stationarity. The more significant ratio is the V75, which adjusts directly the PF based on duration required for steady-state response. Unlike the other corrective ratios, the V75 ratio does not return to unity at low frequencies.

As the magnitude increases, all corrective methods show similar shifts to lower periods due to the longer ground-motion duration. Each of the "rms"-duration methods (i.e., BJ84, LP99, and BT12) show similar albeit slightly different corrective ratios.

While the Boore and Thompson [2015] coefficients are very accurate for the rock parameters used to derive the coefficients—and acceptably accurate for reasonable adjustments to the seismological parameters—they will likely not be accurate for simulations using the full-resonance site-response calculations and equivalent-linear nonlinearity (e.g., Kottke and Rathje [2013]). This is because the coefficients do not account for the increased duration of the oscillator due to site response resonances or substantial changes to the spectral shape. This could be addressed by developing an additional parameter that is a function of the site characteristics to adjust the Boore and Thompson [2014] D_{rms} coefficients. Alternatively, new D_{rms} equations can

be developed that account for the impact of the full-resonance site response on the spectral shape and oscillator duration.

Table 3.1 **The ratios between corrected and uncorrected PF formulations with respect to non-stationarity.**

Corrected	Uncorrected
V75 with n_f	V75 without application of n_f
DK85	D64
CLH56 with BJ84 "rms" duration	CLH56
CLH56 with LP99 "rms" duration	CLH56
CLH56 with BT12 "rms" duration	CLH56

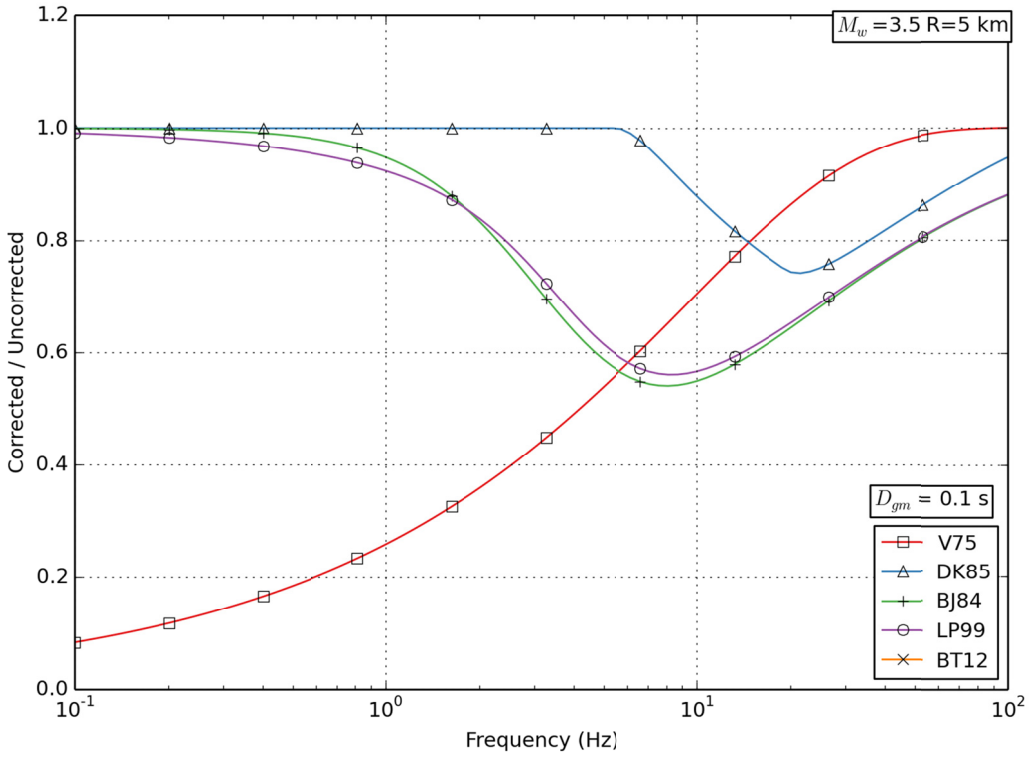

Figure 3.6 **The ratio of the correction to uncorrected oscillator response for the M 3.5 event at a distance of 5 km; see Table 3.1 for the definitions of the corrective ratios.**

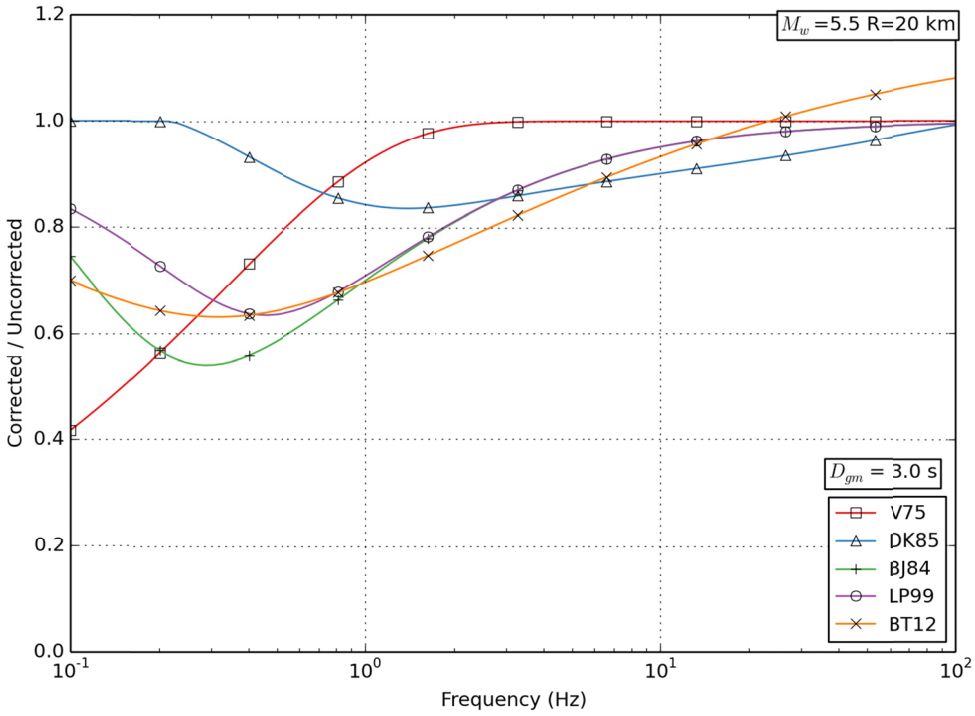

Figure 3.7 **The ratio of the correction to uncorrected oscillator response for the M = 5.5 event at a distance of 20 km; see Table 3.1 for the definitions of the corrective ratios.**

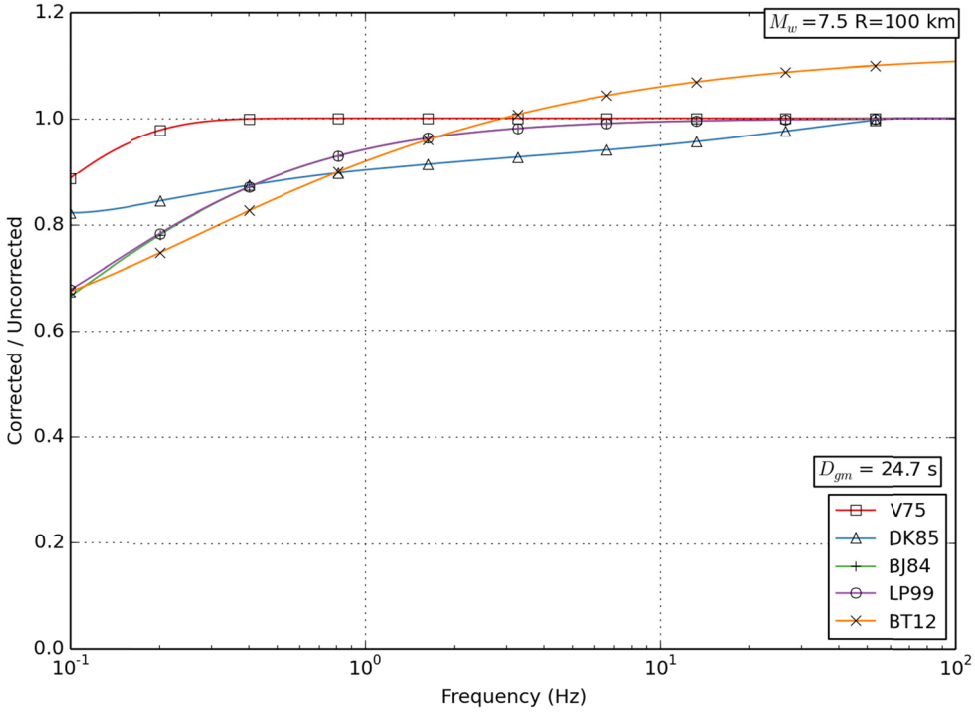

Figure 3.8 **The ratio of the correction to uncorrected oscillator response for the M 7.5 event at a distance of 100 km; see Table 3.1 for the definitions of the corrective ratios.**

4 Processing Ground Motions using the Random Vibration Theory Approach

The records used for ground-motion model (GMM) development per the NGA-East RVT approach (see Chapter 11 by Hollenback et al. in *PEER Report No. 2015/04* for further details on this approach) required additional processing beyond what is described in Goulet et al. [2014]. The two primary additional steps are:

- Definition of an orientation-independent FAS to represent the two as-recorded horizontal components of a record
- Smoothing and down-sampling of the orientation-independent FAS to a reasonable number of frequency points in order to develop a frequency-by-frequency GMM-based FAS

The RVT Working Group's proposed approach for completing these tasks is discussed below.

4.1 ORIENTATION-INDEPENDENT FOURIER AMPLITUDE SPECTRUM

The GMM development (e.g., constraining magnitude scaling and distance attenuation) was performed on the FAS of recorded ground motions. Subsequently, PSA GMMs were defined using this FAS model and a calibrated duration model through RVT. The FAS and duration models were developed from an orientation-independent FAS. We refer to this orientation-independent FAS as the effective amplitude spectrum (EAS), which is defined as

$$\mathrm{EAS}(f) = \sqrt{\frac{1}{2}\left[\mathrm{FAS}_{\mathrm{HC1}}(f)^2 + \mathrm{FAS}_{\mathrm{HC2}}(f)^2\right]} \tag{4.1}$$

where $\mathrm{FAS}_{\mathrm{HC1}}$ and $\mathrm{FAS}_{\mathrm{HC2}}$ are the FAS of first and second as-recorded horizontal components of a three-component time series. By definition, this is independent of the orientation of the instrument. Figures 4.1 and 4.2 compare the FAS of the two as-recorded horizontal components to the EAS for two records from the NGA-East database [Goulet et al. 2014].

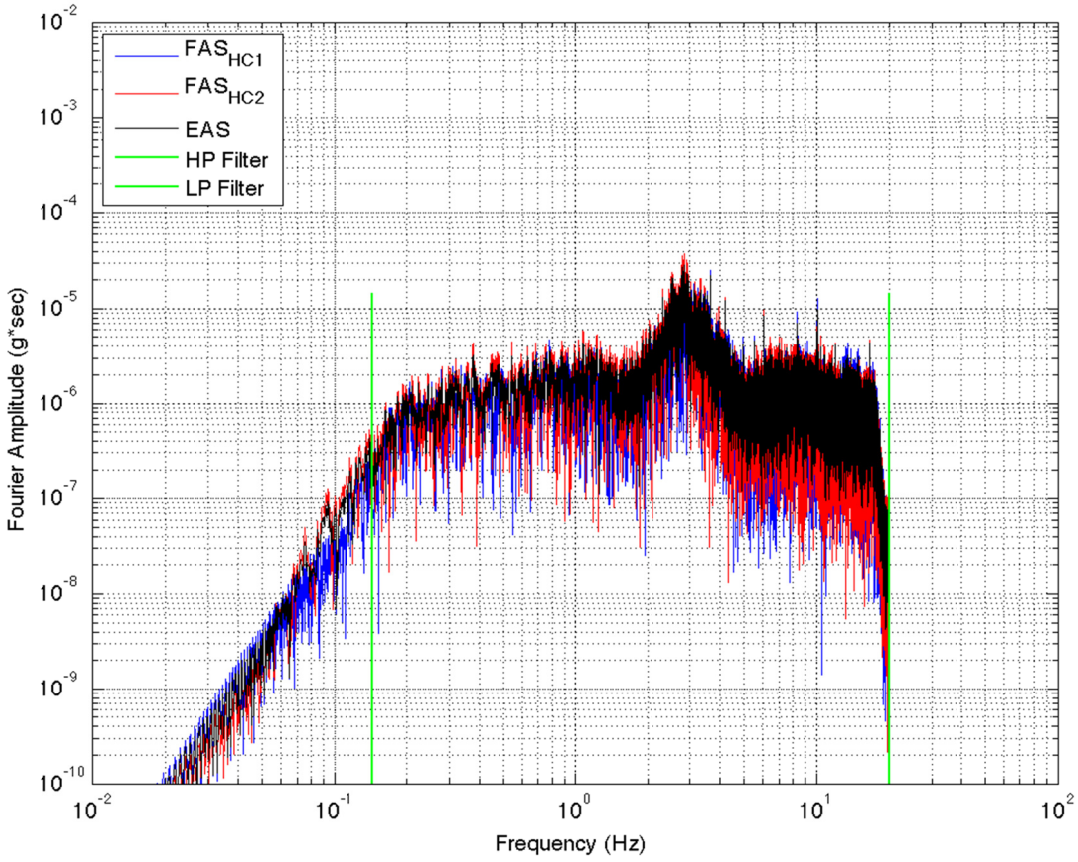

Figure 4.1 **Fourier amplitude spectra from the Cap-Rouge event recorded at station US.GOGA. The north and east components (FASHC1 in blue and FASHC2 in red) are plotted along with the effective amplitude spectrum [Equation (4.1) in black). The green vertical lines represent the high-pass (HP) and low-pass filters (LP) of the record.**

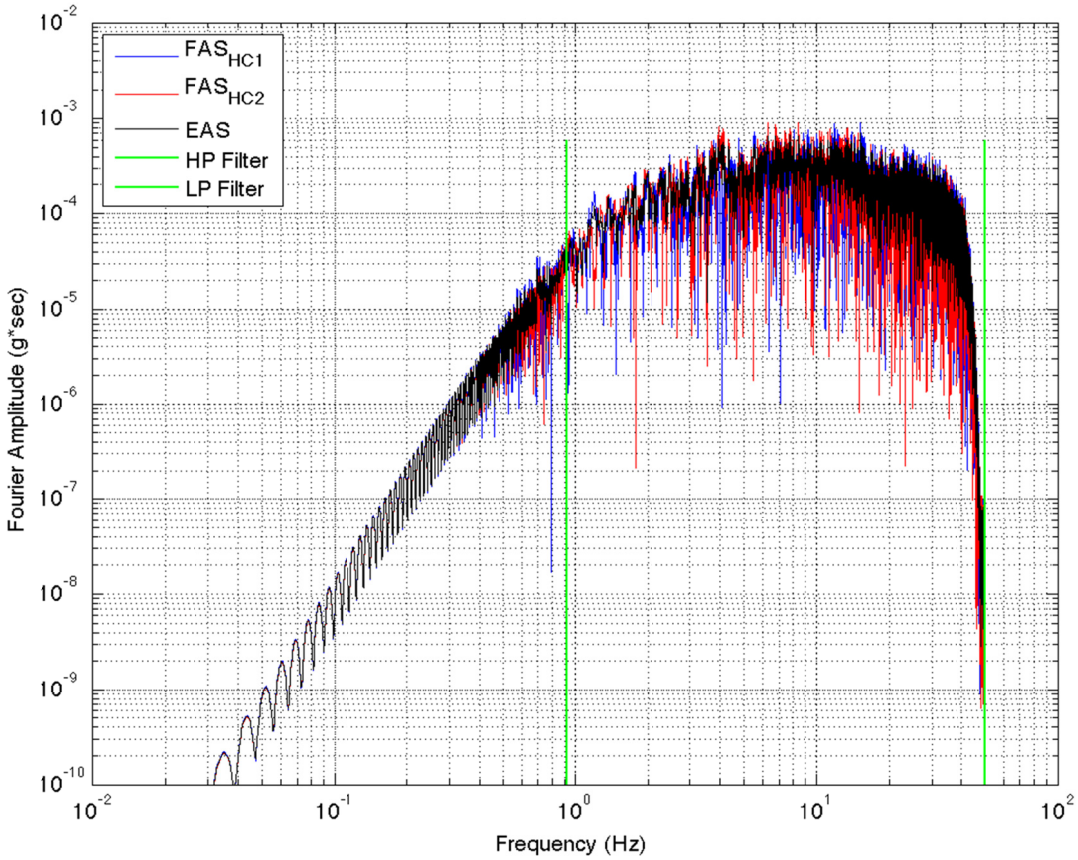

Figure 4.2 **Fourier amplitude spectra from the Cap-Rouge event recorded at station CN.A11 (Station ID 8). The north and east components (FASHC1 in blue and FASHC2 in red) are plotted along with the effective amplitude spectrum (Equation (34), in black). The green vertical lines represent the high-pass (HP) and low-pass filters (LP) of the record.**

4.2 SMOOTHING AND DOWN-SAMPLING

As part of the NGA-East uniform record processing, all time series were padded to longer durations to make the frequency step, Δf, in the FAS as uniform as possible. The choice of Δf was a compromise between record length and reasonably similar Δf, and resulted in the two Δf defined in Table 4.1. This is a departure from other datasets where Δf is defined by the as-recorded record length.

The resulting FAS for these processed records contain very large numbers of frequency points; records with a high Nyquist frequency have over 100,000 frequency points. This is not a practical number of frequencies to use with the NGA-East FAS modeling approach for developing GMMs in which regression is performed frequency-by-frequency. Therefore, all the EAS in the database were uniformly smoothed and down-sampled to a manageable number of frequency points. A wide range of smoothing operators are available, each allowing different

smoothing levels. The smoothing technique and level must be carefully selected so as to not introduce bias relative to the original dataset.

In the context of RVT performed using the Vanmarcke PFs (see Section 2.2.1.3), there are four FAS quantities controlling the process in addition to duration: the *zero*th spectral moment [m_0, Equation (2.4)], δ [a measure of the ground motion band width, Equation (2.14)], the frequency of zero crossings [f_z, Equation (2.5)], and the frequency of extrema [f_e, Equation (2.7)]. The smoothing criterion for the current application was as follows: that the smoothed, down-sampled EAS led to similar quantities as the complete EAS for the four properties relevant to RVT.

Several smoothing windows of various widths were considered and tested, including the Hamming, trapezoidal, and triangular windows. Application of such windows to linear sampling of frequencies led to bias in spectral shape, especially at low frequencies, and did not allow a close match to the four quantities listed above. To prevent these issues, the RVT working group selected the Konno and Ohmachi [1998] (KO) smoothing window, which is based on the log10 sampling of frequencies. The KO window weights are defined by:

$$W(f) = \left\{ \frac{\sin[b \log(f/f_c)]}{b \log(f/f_c)} \right\} \tag{4.2}$$

where W is the weight defined at frequency f for a window centered at frequency f_c and defined by window parameter b. Window parameter b can be defined in terms of the bandwidth in log10 units of the smoothing window as:

$$b = 2\pi / b_w \tag{4.3}$$

where b_w is the bandwidth of the smoothing window in $\log_{10}$ units. The KO smoothing window was selected because it resulted in little-to-no bias on the amplitudes of the smoothed EAS when compared to the unsmoothed EAS. Other smoothing windows considered (the Hamming window, trapezoidal window, and triangular window) did not. Figure 4.3 shows the KO smoothing window for f_c = 5 Hz and four different values of b_w.

Table 4.1 Frequency sampling of the NGA-East dataset.

NGA-East Data	Type 1	Type 2
sps	10, 20, 40	50, 100, 200
dt	0.1, 0.05, 0.025	0.02, 0.01, 0.005
Duration (sec)	3276.8	2621.44
Power of 2	15, 16, 17	17, 18, 19
Δf	0.00030518	0.0003815

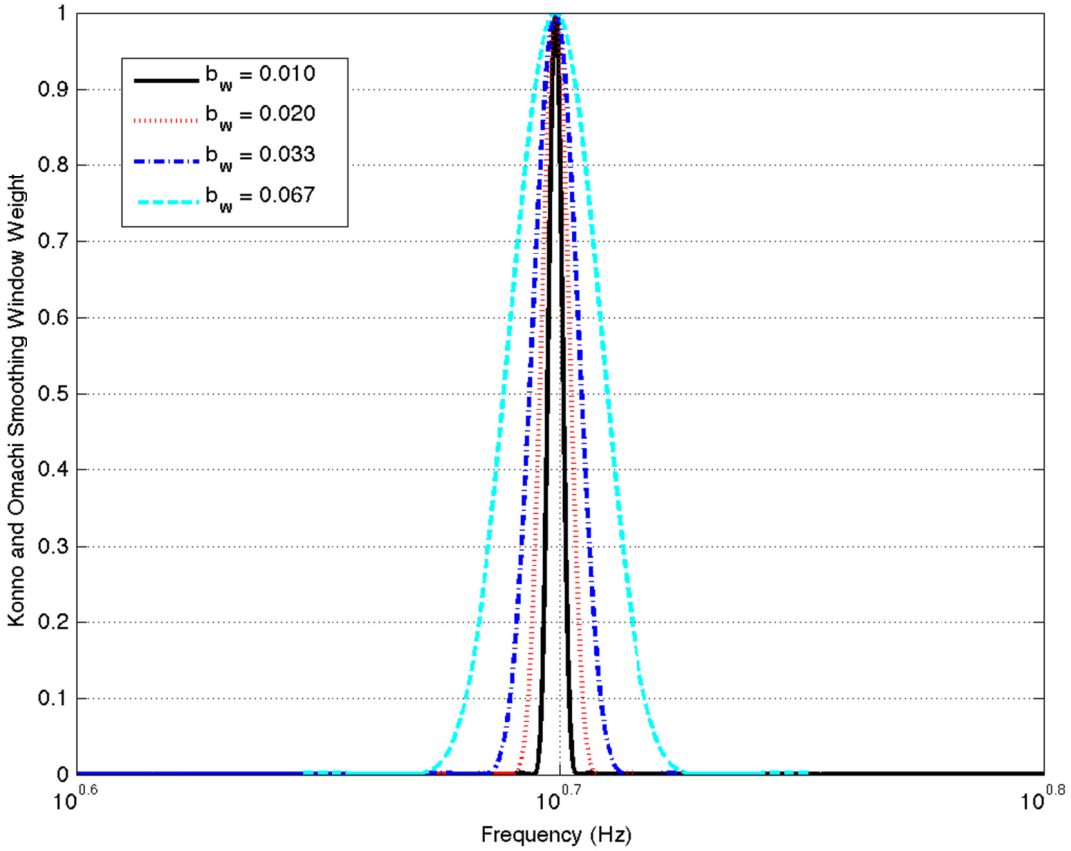

Figure 4.3 **Comparison of Konno and Ohmachi smoothing windows with four different smoothing window bandwidths: 0.01, 0.02, 0.033, and 0.067.**

The four RVT properties selected for calibration are all functions of several different n^{th} order moments of the oscillator frequency response function, which is a function of the square of the FAS of the ground motion. Thus, the smoothing and down-sampling was performed on the square of the EAS in the NGA-East database.

All EAS in NGA-East database were smoothed and down-sampled for six different combinations of smoothing window bandwidth, b_w, and number of frequency points for down-sampling; see Table 4.2. To determine the combination that would have the least impact on subsequent GMM development, the four properties selected for RVT calibration, m_0, q, f_z, and, f_e, were calculated for the original EAS and the smoothed and down-sampled EAS. The comparison was done at three different oscillator periods and covered the full range of periods to be defined by the GMMs: 0.01 sec, 0.2 sec, and 10 sec. The value of each property from the smoothed and down-sampled EAS was compared to that of the original EAS for all the records and each oscillator period. We quantified the number of records in the database whose smoothed and down-sampled RVT properties fell within a given percentage of the original RVT properties. Table 4.2 lists the percentage of records that had smoothed and down-sampled RVT properties that fell within ±1% of original RVT properties. Based on this criteria, the combination of b_w =

1/30 and 100 frequency points per decade was identified as having the least impact on the four RVT calibration properties and were, therefore, selected for smoothing and down-sampling of the NGA-East database. Close inspection of the records falling outside of the 1% range led to the elimination of these records on the basis of a peculiar spectral shape around a limited frequency band. Figures 4.4 and 4.5 compare the original EAS and the smoothed and down-sampled for this selected combination for two different records.

Table 4.2 **Percentage of records in NGA-EAST database that have RVT properties of the smoothed and down-sampled EAS within ±1% of the RVT properties of original EAS.**

Oscillator period = 0.01 sec

Number of frequency points per decade	Width of smoothing window, b_w (fraction of a decade)	m_0	q	f_z	f_e
30	1/15	46%	49%	86%	88%
30	1/30	18%	20%	47%	57%
50	1/30	35%	39%	80%	85%
50	1/50	19%	21%	54%	63%
100	1/30	99%	98%	100%	99%
100	1/100	24%	26%	64%	70%

Oscillator period = 0.2 sec

Number of frequency points per decade	Width of smoothing window, b_w (fraction of a decade)	m_0	q	f_z	f_e
30	1/15	21%	15%	87%	92%
30	1/30	12%	10%	66%	78%
50	1/30	25%	24%	89%	94%
50	1/50	14%	13%	73%	83%
100	1/30	99%	98%	100%	100%
100	1/100	17%	15%	79%	88%

Oscillator period = 10 sec

Number of frequency points per decade	Width of smoothing window, b_w (fraction of a decade)	m_0	q	f_z	f_e
30	1/15	22%	37%	60%	76%
30	1/30	11%	14%	32%	37%
50	1/30	30%	34%	63%	70%
50	1/50	19%	19%	40%	43%
100	1/30	94%	99%	99%	100%
100	1/100	37%	28%	58%	56%

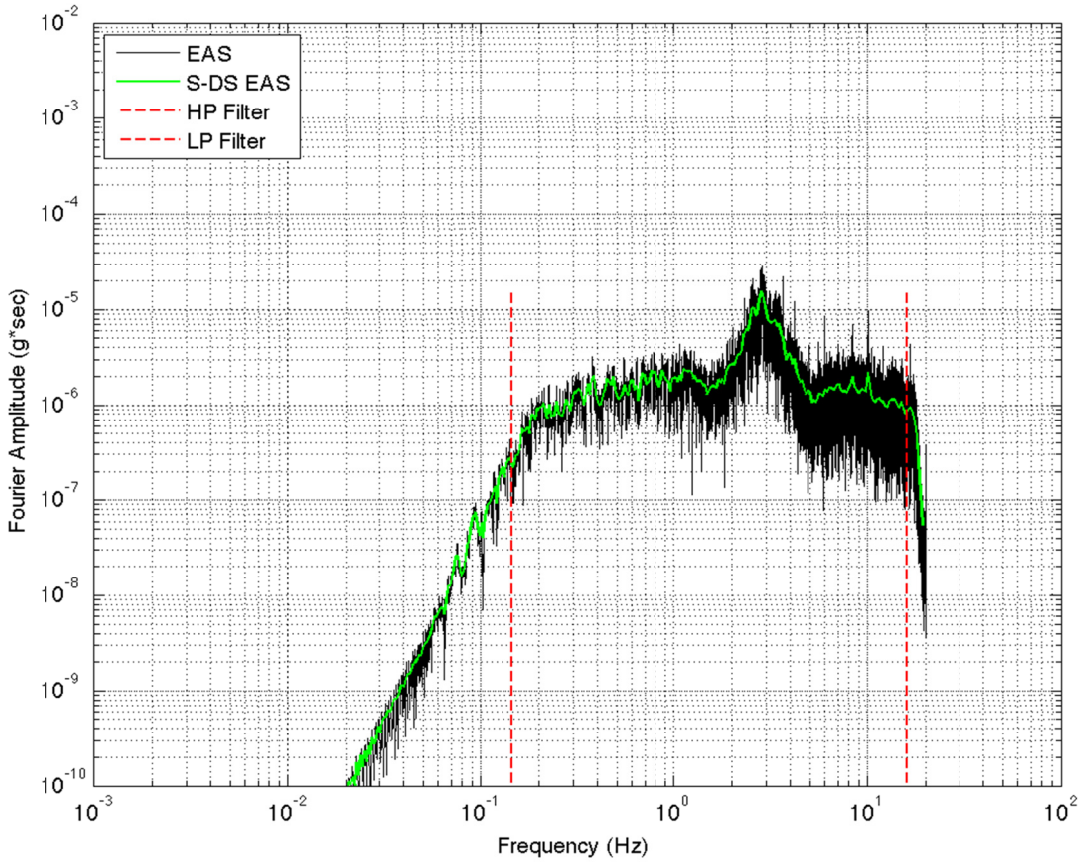

Figure 4.4 **Effective amplitude spectra (EAS) and smoothed and down-sampled effective amplitude spectra (S-DS EAS) from the Cap-Rouge event recorded at station US.GOGA. The red dashed vertical lines represent the high-pass (HP) and low-pass filters (LP) of the record.**

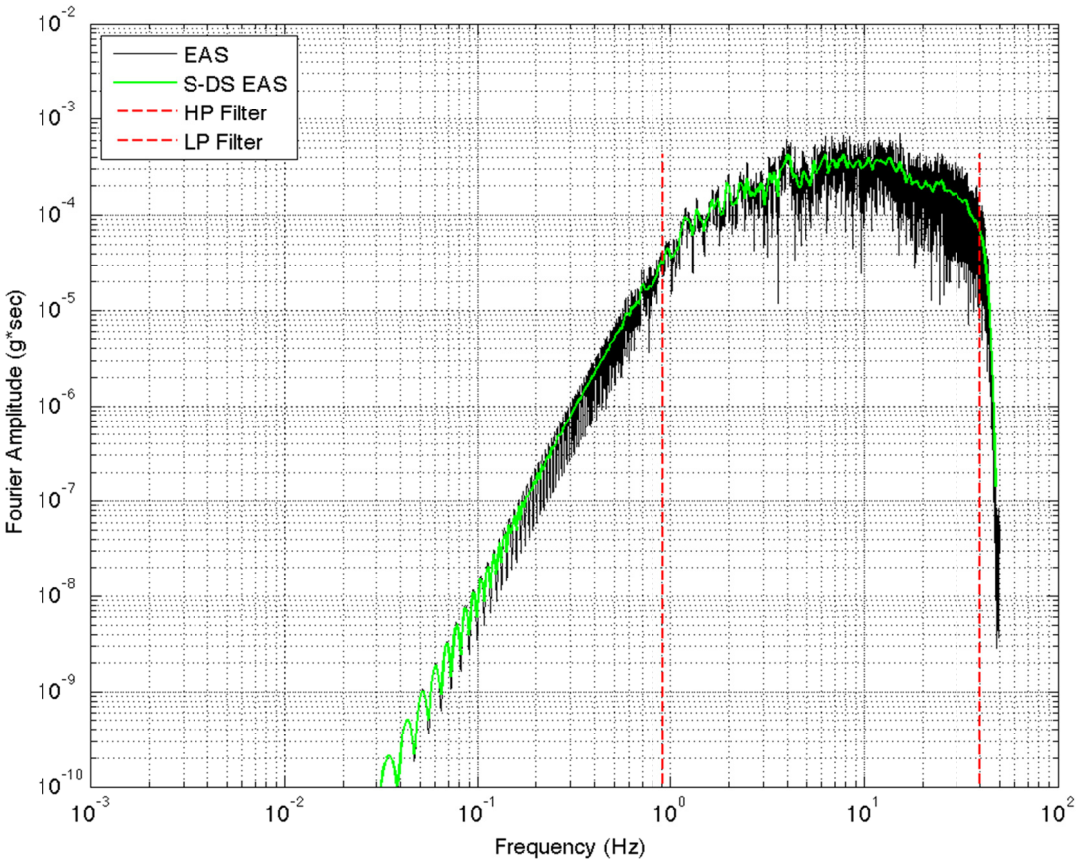

Figure 4.5 **Effective amplitude spectra (EAS) and smoothed and down-sampled effective amplitude spectra (S-DS EAS) from the Cap-Rouge event recorded at station CN.A11. The red dashed vertical lines represent the high-pass (HP) and low-pass filters (LP) of the record.**

5 Conclusions and Future Work

5.1 CONCLUSION: RECOMMENDED APPROACH

This report evaluated the use of RVT for the purpose of median GMM development. Based on their relevance to engineering and seismology communities, two PF formulations are recommended: (1) Cartwright and Longuet-Higgins [1956], and (2) Vanmarcke [1976]. The associated duration corrections developed by Boore and Thompson [2014; 2015] are recommended when response spectra are being computed. Alternatively, new durations optimized to minimize PSA bias could be computed from a region-specific database; that approach, applied to the NGA-East project, is discussed in Chapter 11 of *PEER Report No. 2015/04*.

The orientation-independent FAS referred to as the effective amplitude spectrum (EAS) is recommended to characterize the frequency content of recorded ground motions. Down sampling of the EAS should be done using a Konno and Ohmachi [1998] smoothing window with a width (b_w) of 1/30 and 100 frequency points per decade. Because this smoothing window was identified as having the least impact on the four RVT calibration properties, it was selected for smoothing and down-sampling of the NGA-East database.

This report was originally developed in 2014 for the NGA-East project to document a basis for the ground motion processing and to provide recommendation on the practices for random vibration theory. Since the original draft of this report, there have been additional studies on random vibration theory that are not included in this report, such as: Wang and Rathje [2016]; Wang and Rathje [2018a; 2018b]; and Van Houtte, Larkin, and Holden [2018].

5.2 FUTURE WORK

Several RVT topics were barely touched-on in this report and we identify selected avenues for future research.

1. RVT for site response. Site response studies such as Kottke and Rathje [2013] have demonstrated the potential misfit between TS and RVT site-response analyses. Evaluating RVT for site response is beyond the scope of this document and has not been considered herein. Future work regarding RVT should consider not only how

the method works on simple SDOF oscillators but also on multi-degree of freedom systems (e.g., site response and SDOF oscillators).

2. Host-target corrections. Host-target corrections have been recently used to correct acceleration response spectrum for different site attenuation parameters (e.g., Al Atik et al. [2014]). These correction factors are dependent on the RVT methodology used. Further research needs to be conducted to ensure that the correct factors are not influenced by the PF formulation selected.
3. Applicable frequency range of RVT. The current RVT procedures use a combination of theoretical and empirical corrections to provide accurate estimates of the peak time-domain response. The empirical nature of the correction might cause the RVT results to be accurate only over a select frequency range. This aspect of the empirical corrections has not been well investigated.

REFERENCES

Al Atik L., Kottke A., Abrahamson N.A, Hollenback J. (2014). Kappa (κ) Scaling of ground-motion prediction equations using an inverse random vibration theory approach, *Bull. Seismol. Soc. Am*., 104(1): 336–346.

Atkinson G.M. (1993a). Earthquake source spectra in eastern North America, *Bull. Seismol. Soc. Am*., 83: 1778–1798.

Atkinson G.M. (1993b). Notes on ground motion parameters for eastern North America: duration and H/V ratio, *Bull. Seismol. Soc. Am*., 83: 587–596.

Atkinson, G.M. (1995). Attenuation and source parameters of earthquakes in the Cascadia region, *Bull. Seismol. Soc. Am*., 85: 1327–1342

Atkinson G.M., Boore D.M. (1995). Ground motion relations for eastern North America, *Bull. Seismol. Soc. Am*., 85: 17–30.

Atkinson G.M., Boore D.M. (2006). Earthquake ground-motion prediction equations for eastern North America, *Bull. Seismol. Soc. Am*., 96: 2181–2205. (also see the erratum published in Vol. 97, No. 3, p. 1032).

Atkinson G.M., Silva W.J. (2000). Stochastic modeling of California ground motions, *Bull. Seismol. Soc. Am*., 90: 255–274.

Boore D.M. (1983). Stochastic simulation of high-frequency ground motions based on seismological models of the radiated spectra, *Bull. Seismol. Soc. Am*., 73: 1865–1894.

Boore D.M. (2003). Prediction of ground motion using the stochastic method, *Pure Appl. Geophys*., 160: 635–676.

Boore D.M., Di Alessandro C., Abrahamson N.A. (2014). A generalization of the double-corner-frequency source spectral model and its use in the SCEC BBP Validation Exercise, *Bull. Seismol. Soc. Am*., 104(5): 2387–2398.

Boore D.M., Joyner W.B. (1984). A note on the use of random vibration theory to predict peak amplitudes of transient signals, *Bull. Seismol. Soc. Am*., 74: 2035–2039.

Boore D.M., Thompson E.M. (2012). Empirical improvements for estimating earthquake response spectra with random-vibration theory, *Bull. Seismol. Soc. Am*., 102: 761–772.

Boore D.M., Thompson E.M. (2014). Path durations for use in the stochastic-method simulation of ground motions, *Bull. Seismol. Soc. Am*., 104(5): 2541–2552.

Boore D.M., Thompson E.M. (2015). Revisions to some parameters used in stochastic-method simulations of ground motion, *Bull. Seismol. Soc. Am.,* 105(2a): 1029–1041.

Bora S.S., Scherbaum F., Kuehn N., Stafford P. (2014). Fourier spectral- and duration models for the generation of response spectra adjustable to different source-, propagation-, and site conditions, *Bull. Earthquake Eng*., 12(1): 467–493.

Campbell K.W. (2003). Prediction of strong ground motion using the hybrid empirical method and its use in the development of ground-motion (attenuation) relations in eastern North America, *Bull. Seismol. Soc. Am*., (3): 1012–1033.

Cartwright D.E., Longuet-Higgins M.S. (1956). The statistical distribution of the maxima of a random function, *Proc. R. Soc. London*, 237: 212–232.

Davenport A.G. (1964). Note on the distribution of the largest value of a random function with application to gust loading, *ICE Proc.*, 28(2): 187–196.

Der Kiureghian A. (1980). Structural response to stationary excitation, *J. Eng. Mech. Div*., EM6: 1195–1213.

Goulet C.A., Kishida T. Ancheta T D., Cramer C.H., Darragh R.B., Silva W.J., Hashash Y.M.A., Harmon J., Stewart J.P., Wooddell K.E., Youngs R.R. (2014). PEER NGA-East database, *PEER Report No. 2014/17,* Pacific Earthquake Engineering Research Center, University of California, Berkeley, CA.

Hanks T.C., McGuire R.K. (1981). The character of high-frequency strong ground motion, *Bull. Seismol. Soc. Am*., 71: 2071−2095.

Herrmann R.B. (1985). An extension of random vibration theory estimates of strong ground motion to large distances, *Bull. Seismol. Soc. Am*., 75: 1447−1453.

Konno K., Ohmachi T. (1998). Ground-motion characteristics estimated from spectral ratio between horizontal and vertical components of microtremor, *Bull. Seismol. Soc. Am*., 88(1): 228–241.

Kottke A.R., Rathje E.M. (2013). Comparison of time series and random vibration theory site response methods, *Bull. Seismol. Soc. Am*., 103: 2111−2127.

Liu L., Pezeshk S. (1999). An improvement on the estimation of pseudoresponse spectral velocity using RVT method, *Bull. Seismol. Soc. Am*., 89(5): 1384−1389.

Ou G.-B., Herrmann R.B. (1990). Estimation theory for peak ground motion, *Seismol. Res. Lett.,* 61: 99−107.

Rathje E.M., Kottke A.R., Ozbey M.C. (2005). Using inverse random vibration theory to develop input Fourier amplitude spectra for use in site response, *Proceedings, 16th International Conference on Soil Mechanics and Geotechnical Engineering: TC4 Earthquake Geotechnical Engineering Satellite Conference*, Osaka, Japan, pp. 160−166.

Rathje E.M. (2014). *Personal Communication*.

Saragoni G.R., Hart G.C. (1974). Simulation of artificial earthquakes, *Earthq. Eng. Struct. Dyn*., 2: 249−267.

Toro G.R., McGuire R.K. (1987). An investigation into earthquake ground motion characteristics in eastern North America, *Bull. Seismol. Soc. Am*., 77(2): 468−489.

Trifunac M.D., Brady A.G. (1975). A study on the duration of strong earthquake ground motion, *Bull. Seismol. Soc. Am*., 65: 581−626.

Van Houtte C., Larkin T., Holden C. (2018). On durations, peak factors, and nonstationarity corrections in seismic hazard applications of random vibration theory, *Bull. Seismol. Soc. Am*., 108(1): 418–436.

Vanmarcke E.H. (1975). Distribution of first-passage time for normal stationary random processes, *J. Appl. Mech., Trans., ASME*, 42: 215−220.

Vanmarcke E.H. (1976). Structural response to earthquakes, Chapter 8, C. Lomnitz and E. Rosenblueth (eds.), in: *Seismic Risk and Engineering Decisions*, New York: Elsevier Scientific Pub. Co.

Vanmarcke E.H., Lai S.-S.P. (1980). Strong-motion duration and rms amplitude of earthquake records, *Bull. Seismol. Soc. Am*., 70: 1293–1307.

Wang X., Rathje E.M. (2016). Influence of peak factors on site amplification from random vibration theory based site-response analysis, *Bull. Seismol. Soc. Am*., 106(4): 1733–1746.

Wang X., Rathje E.M. (2018a). Development of ground-motion duration models for use in random vibration theory site-response analysis, *Bull. Seismol. Soc. Am*., 108(4): 2104–2116.

Wang X., Rathje E.M. (2018b). Accounting for changes in duration in random-vibration-theory-based site-response analysis, *Bull. Seismol. Soc. Am*., 108(4): 2117–2129.

Yenier E., Atkinson G.M. (2014). Equivalent point-source modeling of moderate-to-large magnitude earthquakes and associated ground-motion saturation effects, *Bull. Seismol. Soc. Am*., 104(3):1458−1478.

PEER REPORTS

PEER reports are available as a free PDF download from https://peer.berkeley.edu/peer-reports. In addition, printed hard copies of PEER reports can be ordered directly from our printer by following the instructions at https://peer.berkeley.edu/peer-reports. For other related questions about the PEER Report Series, contact the Pacific Earthquake Engineering Research Center, 325 Davis Hall, Mail Code 1792, Berkeley, CA 94720. Tel.: (510) 642-3437; and Email: peer_center@berkeley.edu.

PEER 2018/04 *Capturing Directivity Effects in the Mean and Aleatory Variability of the NGA-West 2 Ground Motion Prediction Equations.* Jennie A. Watson-Lamprey. November 2018.

PEER 2018/03 *Probabilistic Seismic Hazard Analysis Code Verification*. Christie Hale, Norman Abrahamson, and Yousef Bozorgnia. July 2018.

PEER 2018/02 *Update of the BCHydro Subduction Ground-Motion Model using the NGA-Subduction Dataset.* Norman Abrahamson, Nicolas Kuehn, Zeynep Gulerce, Nicholas Gregor, Yousef Bozorgnia, Grace Parker, Jonathan Stewart, Brian Chiou, I. M. Idriss, Kenneth Campbell, and Robert Youngs. June 2018.

PEER 2018/01 *PEER Annual Report 2017–2018*. Khalid Mosalam, Amarnath Kasalanati, and Selim Günay. June 2018.

PEER 2017/12 *Experimental Investigation of the Behavior of Vintage and Retrofit Concentrically Braced Steel Frames under Cyclic Loading*. Barbara G. Simpson, Stephen A. Mahin, and Jiun-Wei Lai, December 2017.

PEER 2017/11 *Preliminary Studies on the Dynamic Response of a Seismically Isolated Prototype Gen-IV Sodium-Cooled Fast Reactor* (*PGSFR*). Benshun Shao, Andreas H. Schellenberg, Matthew J. Schoettler, and Stephen A. Mahin. December 2017.

PEER 2017/10 *Development of Time Histories for IEEE693 Testing and Analysis (including Seismically Isolated Equipment).* Shakhzod M. Takhirov, Eric Fujisaki, Leon Kempner, Michael Riley, and Brian Low. December 2017.

PEER 2017/09 *""R" Package for Computation of Earthquake Ground-Motion Response Spectra.* Pengfei Wang, Jonathan P. Stewart, Yousef Bozorgnia, David M. Boore, and Tadahiro Kishida. December 2017.

PEER 2017/08 *Influence of Kinematic SSI on Foundation Input Motions for Bridges on Deep Foundations*. Benjamin J. Turner, Scott J. Brandenberg, and Jonathan P. Stewart. November 2017.

PEER 2017/07 *A Nonlinear Kinetic Model for Multi-Stage Friction Pendulum Systems*. Paul L. Drazin and Sanjay Govindjee. September 2017.

PEER 2017/06 *Guidelines for Performance-Based Seismic Design of Tall Buildings, Version 2.02*. TBI Working Group led by co-chairs Ron Hamburger and Jack Moehle: Jack Baker, Jonathan Bray, C.B. Crouse, Greg Deierlein, John Hooper, Marshall Lew, Joe Maffei, Stephen Mahin, James Malley, Farzad Naeim, Jonathan Stewart, and John Wallace. May 2017.

PEER 2017/05 *Recommendations for Ergodic Nonlinear Site Amplification in Central and Eastern North America*. Youssef M.A. Hashash, Joseph A. Harmon, Okan Ilhan, Grace A. Parker, and Jonathan P. Stewart. March 2017.

PEER 2017/04 *Expert Panel Recommendations for Ergodic Site Amplification in Central and Eastern North America*. Jonathan P. Stewart, Grace A. Parker, Joseph P. Harmon, Gail M. Atkinson, David M. Boore, Robert B. Darragh, Walter J. Silva, and Youssef M.A. Hashash. March 2017.

PEER 2017/03 *NGA-East Ground-Motion Models for the U.S. Geological Survey National Seismic Hazard Maps*. Christine A. Goulet, Yousef Bozorgnia, Nicolas Kuehn, Linda Al Atik, Robert R. Youngs, Robert W. Graves, and Gail M. Atkinson. March 2017.

PEER 2017/02 *U.S.–New Zealand–Japan Workshop: Liquefaction-Induced Ground Movements Effects, University of California, Berkeley, California, 2–4 November 2016.* Jonathan D. Bray, Ross W. Boulanger, Misko Cubrinovski, Kohji Tokimatsu, Steven L. Kramer, Thomas O'Rourke, Ellen Rathje, Russell A. Green, Peter K. Robinson, and Christine Z. Beyzaei. March 2017.

PEER 2017/01 *2016 PEER Annual Report*. Khalid M. Mosalam, Amarnath Kasalanati, and Grace Kang. March 2017.

PEER 2016/10 *Performance-Based Robust Nonlinear Seismic Analysis with Application to Reinforced Concrete Bridge Systems*. Xiao Ling and Khalid M. Mosalam. December 2016.

PEER 2017/09 *Segmental Displacement Control Design for Seismically Isolated Bridges,* Kenneth A. Ogorzalek and Stephen A. Mahin. December 2016.

PEER 2016/08 *Resilience of Critical Structures, Infrastructure, and Communities*. Gian Paolo Cimellaro, Ali Zamani-Noori, Omar Kamouh, Vesna Terzic, and Stephen A. Mahin. December 2016.

PEER 2016/07 *Hybrid Simulation Theory for a Classical Nonlinear Dynamical System*. Paul L. Drazin and Sanjay Govindjee. September 2016.

PEER 2016/06 *California Earthquake Early Warning System Benefit Study*. Laurie A. Johnson, Sharyl Rabinovici, Grace S. Kang, and Stephen A. Mahin. July 2006.

PEER 2016/05 *Ground-Motion Prediction Equations for Arias Intensity Consistent with the NGA-West2 Ground-Motion Models.* Charlotte Abrahamson, Hao-Jun Michael Shi, and Brian Yang. July 2016.

PEER 2016/04 *The M_W 6.0 South Napa Earthquake of August 24, 2014: A Wake-Up Call for Renewed Investment in Seismic Resilience Across California.* Prepared for the California Seismic Safety Commission, Laurie A. Johnson and Stephen A. Mahin. May 2016.

PEER 2016/03 *Simulation Confidence in Tsunami-Driven Overland Flow.* Patrick Lynett. May 2016.

PEER 2016/02 *Semi-Automated Procedure for Windowing time Series and Computing Fourier Amplitude Spectra for the NGA-West2 Database.* Tadahiro Kishida, Olga-Joan Ktenidou, Robert B. Darragh, and Walter J. Silva. May 2016.

PEER 2016/01 *A Methodology for the Estimation of Kappa (κ) from Large Datasets: Example Application to Rock Sites in the NGA-East Database and Implications on Design Motions.* Olga-Joan Ktenidou, Norman A. Abrahamson, Robert B. Darragh, and Walter J. Silva. April 2016.

PEER 2015/13 *Self-Centering Precast Concrete Dual-Steel-Shell Columns for Accelerated Bridge Construction: Seismic Performance, Analysis, and Design*. Gabriele Guerrini, José I. Restrepo, Athanassios Vervelidis, and Milena Massari. December 2015.

PEER 2015/12 *Shear-Flexure Interaction Modeling for Reinforced Concrete Structural Walls and Columns under Reversed Cyclic Loading*. Kristijan Kolozvari, Kutay Orakcal, and John Wallace. December 2015.

PEER 2015/11 *Selection and Scaling of Ground Motions for Nonlinear Response History Analysis of Buildings in Performance-Based Earthquake Engineering*. N. Simon Kwong and Anil K. Chopra. December 2015.

PEER 2015/10 *Structural Behavior of Column-Bent Cap Beam-Box Girder Systems in Reinforced Concrete Bridges Subjected to Gravity and Seismic Loads. Part II: Hybrid Simulation and Post-Test Analysis*. Mohamed A. Moustafa and Khalid M. Mosalam. November 2015.

PEER 2015/09 *Structural Behavior of Column-Bent Cap Beam-Box Girder Systems in Reinforced Concrete Bridges Subjected to Gravity and Seismic Loads. Part I: Pre-Test Analysis and Quasi-Static Experiments*. Mohamed A. Moustafa and Khalid M. Mosalam. September 2015.

PEER 2015/08 *NGA-East: Adjustments to Median Ground-Motion Models for Center and Eastern North America*. August 2015.

PEER 2015/07 *NGA-East: Ground-Motion Standard-Deviation Models for Central and Eastern North America*. Linda Al Atik. June 2015.

PEER 2015/06 *Adjusting Ground-Motion Intensity Measures to a Reference Site for which V_{S30} = 3000 m/sec*. David M. Boore. May 2015.

PEER 2015/05 *Hybrid Simulation of Seismic Isolation Systems Applied to an APR-1400 Nuclear Power Plant.* Andreas H. Schellenberg, Alireza Sarebanha, Matthew J. Schoettler, Gilberto Mosqueda, Gianmario Benzoni, and Stephen A. Mahin. April 2015.

PEER 2015/04 *NGA-East: Median Ground-Motion Models for the Central and Eastern North America Region*. April 2015.

PEER 2015/03 *Single Series Solution for the Rectangular Fiber-Reinforced Elastomeric Isolator Compression Modulus*. James M. Kelly and Niel C. Van Engelen. March 2015.

PEER 2015/02 *A Full-Scale, Single-Column Bridge Bent Tested by Shake-Table Excitation.* Matthew J. Schoettler, José I. Restrepo, Gabriele Guerrini, David E. Duck, and Francesco Carrea. March 2015.

PEER 2015/01 *Concrete Column Blind Prediction Contest 2010: Outcomes and Observations.* Vesna Terzic, Matthew J. Schoettler, José I. Restrepo, and Stephen A Mahin. March 2015.

PEER 2014/20 *Stochastic Modeling and Simulation of Near-Fault Ground Motions for Performance-Based Earthquake Engineering*. Mayssa Dabaghi and Armen Der Kiureghian. December 2014.

PEER 2014/19 *Seismic Response of a Hybrid Fiber-Reinforced Concrete Bridge Column Detailed for Accelerated Bridge Construction*. Wilson Nguyen, William Trono, Marios Panagiotou, and Claudia P. Ostertag. December 2014.

PEER 2014/18 *Three-Dimensional Beam-Truss Model for Reinforced Concrete Walls and Slabs Subjected to Cyclic Static or Dynamic Loading*. Yuan Lu, Marios Panagiotou, and Ioannis Koutromanos. December 2014.

PEER 2014/17 *PEER NGA-East Database*. Christine A. Goulet, Tadahiro Kishida, Timothy D. Ancheta, Chris H. Cramer, Robert B. Darragh, Walter J. Silva, Youssef M.A. Hashash, Joseph Harmon, Jonathan P. Stewart, Katie E. Wooddell, and Robert R. Youngs. October 2014.

PEER 2014/16 *Guidelines for Performing Hazard-Consistent One-Dimensional Ground Response Analysis for Ground Motion Prediction*. Jonathan P. Stewart, Kioumars Afshari, and Youssef M.A. Hashash. October 2014.

PEER 2014/15 *NGA-East Regionalization Report: Comparison of Four Crustal Regions within Central and Eastern North America using Waveform Modeling and 5%-Damped Pseudo-Spectral Acceleration Response*. Jennifer Dreiling, Marius P. Isken, Walter D. Mooney, Martin C. Chapman, and Richard W. Godbee. October 2014.

PEER 2014/14 *Scaling Relations between Seismic Moment and Rupture Area of Earthquakes in Stable Continental Regions*. Paul Somerville. August 2014.

PEER 2014/13 *PEER Preliminary Notes and Observations on the August 24, 2014, South Napa Earthquake*. Grace S. Kang and Stephen A. Mahin, Editors. September 2014.

PEER 2014/12 *Reference-Rock Site Conditions for Central and Eastern North America: Part II – Attenuation (Kappa) Definition*. Kenneth W. Campbell, Youssef M.A. Hashash, Byungmin Kim, Albert R. Kottke, Ellen M. Rathje, Walter J. Silva, and Jonathan P. Stewart. August 2014.

PEER 2014/11 *Reference-Rock Site Conditions for Central and Eastern North America: Part I - Velocity Definition*. Youssef M.A. Hashash, Albert R. Kottke, Jonathan P. Stewart, Kenneth W. Campbell, Byungmin Kim, Ellen M. Rathje, Walter J. Silva, Sissy Nikolaou, and Cheryl Moss. August 2014.

PEER 2014/10 *Evaluation of Collapse and Non-Collapse of Parallel Bridges Affected by Liquefaction and Lateral Spreading*. Benjamin Turner, Scott J. Brandenberg, and Jonathan P. Stewart. August 2014.

PEER 2014/09 *PEER Arizona Strong-Motion Database and GMPEs Evaluation*. Tadahiro Kishida, Robert E. Kayen, Olga-Joan Ktenidou, Walter J. Silva, Robert B. Darragh, and Jennie Watson-Lamprey. June 2014.

PEER 2014/08 *Unbonded Pretensioned Bridge Columns with Rocking Detail*. Jeffrey A. Schaefer, Bryan Kennedy, Marc O. Eberhard, and John F. Stanton. June 2014.

PEER 2014/07 *Northridge 20 Symposium Summary Report: Impacts, Outcomes, and Next Steps*. May 2014.

PEER 2014/06 *Report of the Tenth Planning Meeting of NEES/E-Defense Collaborative Research on Earthquake Engineering*. December 2013.

PEER 2014/05 *Seismic Velocity Site Characterization of Thirty-One Chilean Seismometer Stations by Spectral Analysis of Surface Wave Dispersion*. Robert Kayen, Brad D. Carkin, Skye Corbet, Camilo Pinilla, Allan Ng, Edward Gorbis, and Christine Truong. April 2014.

PEER 2014/04 Effect of Vertical Acceleration on Shear Strength of Reinforced Concrete Columns. Hyerin Lee and Khalid M. Mosalam. April 2014.

PEER 2014/03 *Retest of Thirty-Year-Old Neoprene Isolation Bearings.* James M. Kelly and Niel C. Van Engelen. March 2014.

PEER 2014/02 *Theoretical Development of Hybrid Simulation Applied to Plate Structures.* Ahmed A. Bakhaty, Khalid M. Mosalam, and Sanjay Govindjee. January 2014.

PEER 2014/01 *Performance-Based Seismic Assessment of Skewed Bridges.* Peyman Kaviani, Farzin Zareian, and Ertugrul Taciroglu. January 2014.

PEER 2013/26 *Urban Earthquake Engineerin*g. Proceedings of the U.S.-Iran Seismic Workshop. December 2013.

PEER 2013/25 *Earthquake Engineering for Resilient Communities: 2013 PEER Internship Program Research Report Collection.* Heidi Tremayne (Editor), Stephen A. Mahin (Editor), Jorge Archbold Monterossa, Matt Brosman, Shelly Dean, Katherine deLaveaga, Curtis Fong, Donovan Holder, Rakeeb Khan, Elizabeth Jachens, David Lam, Daniela Martinez Lopez, Mara Minner, Geffen Oren, Julia Pavicic, Melissa Quinonez, Lorena Rodriguez, Sean Salazar, Kelli Slaven, Vivian Steyert, Jenny Taing, and Salvador Tena. December 2013.

PEER 2013/24 *NGA-West2 Ground Motion Prediction Equations for Vertical Ground Motions*. September 2013.

PEER 2013/23 *Coordinated Planning and Preparedness for Fire Following Major Earthquakes*. Charles Scawthorn. November 2013.

PEER 2013/22 *GEM-PEER Task 3 Project: Selection of a Global Set of Ground Motion Prediction Equations.* Jonathan P. Stewart, John Douglas, Mohammad B. Javanbarg, Carola Di Alessandro, Yousef Bozorgnia, Norman A. Abrahamson, David M. Boore, Kenneth W. Campbell, Elise Delavaud, Mustafa Erdik, and Peter J. Stafford. December 2013.

PEER 2013/21 *Seismic Design and Performance of Bridges with Columns on Rocking Foundations*. Grigorios Antonellis and Marios Panagiotou. September 2013.

PEER 2013/20 *Experimental and Analytical Studies on the Seismic Behavior of Conventional and Hybrid Braced Frames*. Jiun-Wei Lai and Stephen A. Mahin. September 2013.

PEER 2013/19 *Toward Resilient Communities: A Performance-Based Engineering Framework for Design and Evaluation of the Built Environment.* Michael William Mieler, Bozidar Stojadinovic, Robert J. Budnitz, Stephen A. Mahin, and Mary C. Comerio. September 2013.

PEER 2013/18 *Identification of Site Parameters that Improve Predictions of Site Amplification*. Ellen M. Rathje and Sara Navidi. July 2013.

PEER 2013/17 *Response Spectrum Analysis of Concrete Gravity Dams Including Dam-Water-Foundation Interaction*. Arnkjell Løkke and Anil K. Chopra. July 2013.

PEER 2013/16 *Effect of Hoop Reinforcement Spacing on the Cyclic Response of Large Reinforced Concrete Special Moment Frame Beams.* Marios Panagiotou, Tea Visnjic, Grigorios Antonellis, Panagiotis Galanis, and Jack P. Moehle. June 2013.

PEER 2013/15 *A Probabilistic Framework to Include the Effects of Near-Fault Directivity in Seismic Hazard Assessment*. Shrey Kumar Shahi, Jack W. Baker. October 2013.

PEER 2013/14 *Hanging-Wall Scaling using Finite-Fault Simulations.* Jennifer L. Donahue and Norman A. Abrahamson. September 2013.

PEER 2013/13 *Semi-Empirical Nonlinear Site Amplification and its Application in NEHRP Site Factors*. Jonathan P. Stewart and Emel Seyhan. November 2013.

PEER 2013/12 *Nonlinear Horizontal Site Response for the NGA-West2 Project.* Ronnie Kamai, Norman A. Abramson, Walter J. Silva. May 2013.

PEER 2013/11 *Epistemic Uncertainty for NGA-West2 Models.* Linda Al Atik and Robert R. Youngs. May 2013.

PEER 2013/10 *NGA-West 2 Models for Ground-Motion Directionality.* Shrey K. Shahi and Jack W. Baker. May 2013.

PEER 2013/09 *Final Report of the NGA-West2 Directivity Working Group.* Paul Spudich, Jeffrey R. Bayless, Jack W. Baker, Brian S.J. Chiou, Badie Rowshandel, Shrey Shahi, and Paul Somerville. May 2013.

PEER 2013/08 *NGA-West2 Model for Estimating Average Horizontal Values of Pseudo-Absolute Spectral Accelerations Generated by Crustal Earthquakes*. I. M. Idriss. May 2013.

PEER 2013/07 *Update of the Chiou and Youngs NGA Ground Motion Model for Average Horizontal Component of Peak Ground Motion and Response Spectra*. Brian Chiou and Robert Youngs. May 2013.

PEER 2013/06 *NGA-West2 Campbell-Bozorgnia Ground Motion Model for the Horizontal Components of PGA, PGV, and 5%-Damped Elastic Pseudo-Acceleration Response Spectra for Periods Ranging from 0.01 to 10 sec.* Kenneth W. Campbell and Yousef Bozorgnia. May 2013.

PEER 2013/05 *NGA-West 2 Equations for Predicting Response Spectral Accelerations for Shallow Crustal Earthquakes*. David M. Boore, Jonathan P. Stewart, Emel Seyhan, and Gail M. Atkinson. May 2013.

PEER 2013/04 *Update of the AS08 Ground-Motion Prediction Equations Based on the NGA-West2 Data Set*. Norman Abrahamson, Walter Silva, and Ronnie Kamai. May 2013.

PEER 2013/03 *PEER NGA-West2 Database.* Timothy D. Ancheta, Robert B. Darragh, Jonathan P. Stewart, Emel Seyhan, Walter J. Silva, Brian S.J. Chiou, Katie E. Wooddell, Robert W. Graves, Albert R. Kottke, David M. Boore, Tadahiro Kishida, and Jennifer L. Donahue. May 2013.

PEER 2013/02 *Hybrid Simulation of the Seismic Response of Squat Reinforced Concrete Shear Walls*. Catherine A. Whyte and Bozidar Stojadinovic. May 2013.

PEER 2013/01 *Housing Recovery in Chile: A Qualitative Mid-program Review*. Mary C. Comerio. February 2013.

PEER 2012/08 *Guidelines for Estimation of Shear Wave Velocity.* Bernard R. Wair, Jason T. DeJong, and Thomas Shantz. December 2012.

PEER 2012/07 *Earthquake Engineering for Resilient Communities: 2012 PEER Internship Program Research Report Collection.* Heidi Tremayne (Editor), Stephen A. Mahin (Editor), Collin Anderson, Dustin Cook, Michael Erceg, Carlos Esparza, Jose Jimenez, Dorian Krausz, Andrew Lo, Stephanie Lopez, Nicole McCurdy, Paul Shipman, Alexander Strum, Eduardo Vega. December 2012.

PEER 2012/06 *Fragilities for Precarious Rocks at Yucca Mountain.* Matthew D. Purvance, Rasool Anooshehpoor, and James N. Brune. December 2012.

PEER 2012/05 *Development of Simplified Analysis Procedure for Piles in Laterally Spreading Layered Soils.* Christopher R. McGann, Pedro Arduino, and Peter Mackenzie–Helnwein. December 2012.

PEER 2012/04 *Unbonded Pre-Tensioned Columns for Bridges in Seismic Regions.* Phillip M. Davis, Todd M. Janes, Marc O. Eberhard, and John F. Stanton. December 2012.

PEER 2012/03 *Experimental and Analytical Studies on Reinforced Concrete Buildings with Seismically Vulnerable Beam-Column Joints*. Sangjoon Park and Khalid M. Mosalam. October 2012.

PEER 2012/02 *Seismic Performance of Reinforced Concrete Bridges Allowed to Uplift during Multi-Directional Excitation*. Andres Oscar Espinoza and Stephen A. Mahin. July 2012.

PEER 2012/01 *Spectral Damping Scaling Factors for Shallow Crustal Earthquakes in Active Tectonic Regions.* Sanaz Rezaeian, Yousef Bozorgnia, I. M. Idriss, Kenneth Campbell, Norman Abrahamson, and Walter Silva. July 2012.

PEER 2011/10 *Earthquake Engineering for Resilient Communities: 2011 PEER Internship Program Research Report Collection*. Heidi Faison and Stephen A. Mahin, Editors. December 2011.

PEER 2011/09 *Calibration of Semi-Stochastic Procedure for Simulating High-Frequency Ground Motions*. Jonathan P. Stewart, Emel Seyhan, and Robert W. Graves. December 2011.

PEER 2011/08 *Water Supply in regard to Fire Following Earthquake*. Charles Scawthorn. November 2011.

PEER 2011/07 *Seismic Risk Management in Urban Areas*. Proceedings of a U.S.-Iran-Turkey Seismic Workshop. September 2011.

PEER 2011/06 *The Use of Base Isolation Systems to Achieve Complex Seismic Performance Objectives*. Troy A. Morgan and Stephen A. Mahin. July 2011.

PEER 2011/05 *Case Studies of the Seismic Performance of Tall Buildings Designed by Alternative Means.* Task 12 Report for the Tall Buildings Initiative. Jack Moehle, Yousef Bozorgnia, Nirmal Jayaram, Pierson Jones, Mohsen Rahnama, Nilesh Shome, Zeynep Tuna, John Wallace, Tony Yang, and Farzin Zareian. July 2011.

PEER 2011/04 *Recommended Design Practice for Pile Foundations in Laterally Spreading Ground.* Scott A. Ashford, Ross W. Boulanger, and Scott J. Brandenberg. June 2011.

PEER 2011/03 *New Ground Motion Selection Procedures and Selected Motions for the PEER Transportation Research Program*. Jack W. Baker, Ting Lin, Shrey K. Shahi, and Nirmal Jayaram. March 2011.

PEER 2011/02 *A Bayesian Network Methodology for Infrastructure Seismic Risk Assessment and Decision Support*. Michelle T. Bensi, Armen Der Kiureghian, and Daniel Straub. March 2011.

PEER 2011/01 *Demand Fragility Surfaces for Bridges in Liquefied and Laterally Spreading Ground.* Scott J. Brandenberg, Jian Zhang, Pirooz Kashighandi, Yili Huo, and Minxing Zhao. March 2011.

PEER 2010/05 *Guidelines for Performance-Based Seismic Design of Tall Buildings.* Developed by the Tall Buildings Initiative. November 2010.

PEER 2010/04 *Application Guide for the Design of Flexible and Rigid Bus Connections between Substation Equipment Subjected to Earthquakes.* Jean-Bernard Dastous and Armen Der Kiureghian. September 2010.

PEER 2010/03 *Shear Wave Velocity as a Statistical Function of Standard Penetration Test Resistance and Vertical Effective Stress at Caltrans Bridge Sites.* Scott J. Brandenberg, Naresh Bellana, and Thomas Shantz. June 2010.

PEER 2010/02 *Stochastic Modeling and Simulation of Ground Motions for Performance-Based Earthquake Engineering.* Sanaz Rezaeian and Armen Der Kiureghian. June 2010.

PEER 2010/01 *Structural Response and Cost Characterization of Bridge Construction Using Seismic Performance Enhancement Strategies.* Ady Aviram, Božidar Stojadinović, Gustavo J. Parra-Montesinos, and Kevin R. Mackie. March 2010.

PEER 2009/03 *The Integration of Experimental and Simulation Data in the Study of Reinforced Concrete Bridge Systems Including Soil-Foundation-Structure Interaction.* Matthew Dryden and Gregory L. Fenves. November 2009.

PEER 2009/02 *Improving Earthquake Mitigation through Innovations and Applications in Seismic Science, Engineering, Communication, and Response*. Proceedings of a U.S.-Iran Seismic Workshop. October 2009.

PEER 2009/01 *Evaluation of Ground Motion Selection and Modification Methods: Predicting Median Interstory Drift Response of Buildings*. Curt B. Haselton, Editor. June 2009.

PEER 2008/10 *Technical Manual for Strata.* Albert R. Kottke and Ellen M. Rathje. February 2009.

PEER 2008/09 *NGA Model for Average Horizontal Component of Peak Ground Motion and Response Spectra.* Brian S.-J. Chiou and Robert R. Youngs. November 2008.

PEER 2008/08 *Toward Earthquake-Resistant Design of Concentrically Braced Steel Structures*. Patxi Uriz and Stephen A. Mahin. November 2008.

PEER 2008/07 *Using OpenSees for Performance-Based Evaluation of Bridges on Liquefiable Soils*. Stephen L. Kramer, Pedro Arduino, and HyungSuk Shin. November 2008.

PEER 2008/06 *Shaking Table Tests and Numerical Investigation of Self-Centering Reinforced Concrete Bridge Columns*. Hyung IL Jeong, Junichi Sakai, and Stephen A. Mahin. September 2008.

PEER 2008/05 *Performance-Based Earthquake Engineering Design Evaluation Procedure for Bridge Foundations Undergoing Liquefaction-Induced Lateral Ground Displacement*. Christian A. Ledezma and Jonathan D. Bray. August 2008.

PEER 2008/04 *Benchmarking of Nonlinear Geotechnical Ground Response Analysis Procedures.* Jonathan P. Stewart, Annie On-Lei Kwok, Youssef M. A. Hashash, Neven Matasovic, Robert Pyke, Zhiliang Wang, and Zhaohui Yang. August 2008.

PEER 2008/03 *Guidelines for Nonlinear Analysis of Bridge Structures in California.* Ady Aviram, Kevin R. Mackie, and Božidar Stojadinović. August 2008.

PEER 2008/02 *Treatment of Uncertainties in Seismic-Risk Analysis of Transportation Systems*. Evangelos Stergiou and Anne S. Kiremidjian. July 2008.

PEER 2008/01 *Seismic Performance Objectives for Tall Buildings.* William T. Holmes, Charles Kircher, William Petak, and Nabih Youssef. August 2008.

PEER 2007/12 *An Assessment to Benchmark the Seismic Performance of a Code-Conforming Reinforced Concrete Moment-Frame Building.* Curt Haselton, Christine A. Goulet, Judith Mitrani-Reiser, James L. Beck, Gregory G. Deierlein, Keith A. Porter, Jonathan P. Stewart, and Ertugrul Taciroglu. August 2008.

PEER 2007/11 *Bar Buckling in Reinforced Concrete Bridge Columns.* Wayne A. Brown, Dawn E. Lehman, and John F. Stanton. February 2008.

PEER 2007/10 *Computational Modeling of Progressive Collapse in Reinforced Concrete Frame Structures*. Mohamed M. Talaat and Khalid M. Mosalam. May 2008.

PEER 2007/09 *Integrated Probabilistic Performance-Based Evaluation of Benchmark Reinforced Concrete Bridges*. Kevin R. Mackie, John-Michael Wong, and Božidar Stojadinović. January 2008.

PEER 2007/08 *Assessing Seismic Collapse Safety of Modern Reinforced Concrete Moment-Frame Buildings*. Curt B. Haselton and Gregory G. Deierlein. February 2008.

PEER 2007/07 *Performance Modeling Strategies for Modern Reinforced Concrete Bridge Columns*. Michael P. Berry and Marc O. Eberhard. April 2008.

PEER 2007/06 *Development of Improved Procedures for Seismic Design of Buried and Partially Buried Structures*. Linda Al Atik and Nicholas Sitar. June 2007.

PEER 2007/05 *Uncertainty and Correlation in Seismic Risk Assessment of Transportation Systems*. Renee G. Lee and Anne S. Kiremidjian. July 2007.

PEER 2007/04 *Numerical Models for Analysis and Performance-Based Design of Shallow Foundations Subjected to Seismic Loading.* Sivapalan Gajan, Tara C. Hutchinson, Bruce L. Kutter, Prishati Raychowdhury, José A. Ugalde, and Jonathan P. Stewart. May 2008.

PEER 2007/03 *Beam-Column Element Model Calibrated for Predicting Flexural Response Leading to Global Collapse of RC Frame Buildings*. Curt B. Haselton, Abbie B. Liel, Sarah Taylor Lange, and Gregory G. Deierlein. May 2008.

PEER 2007/02 *Campbell-Bozorgnia NGA Ground Motion Relations for the Geometric Mean Horizontal Component of Peak and Spectral Ground Motion Parameters*. Kenneth W. Campbell and Yousef Bozorgnia. May 2007.

PEER 2007/01 *Boore-Atkinson NGA Ground Motion Relations for the Geometric Mean Horizontal Component of Peak and Spectral Ground Motion Parameters*. David M. Boore and Gail M. Atkinson. May 2007.

PEER 2006/12 Societal Implications of Performance-Based Earthquake Engineering. Peter J. May. May 2007.

PEER 2006/11 *Probabilistic Seismic Demand Analysis Using Advanced Ground Motion Intensity Measures, Attenuation Relationships, and Near-Fault Effects*. Polsak Tothong and C. Allin Cornell. March 2007.

PEER 2006/10 *Application of the PEER PBEE Methodology to the I-880 Viaduct*. Sashi Kunnath. February 2007.

PEER 2006/09 *Quantifying Economic Losses from Travel Forgone Following a Large Metropolitan Earthquake*. James Moore, Sungbin Cho, Yue Yue Fan, and Stuart Werner. November 2006.

PEER 2006/08 *Vector-Valued Ground Motion Intensity Measures for Probabilistic Seismic Demand Analysis*. Jack W. Baker and C. Allin Cornell. October 2006.

PEER 2006/07 *Analytical Modeling of Reinforced Concrete Walls for Predicting Flexural and Coupled–Shear-Flexural Responses*. Kutay Orakcal, Leonardo M. Massone, and John W. Wallace. October 2006.

PEER 2006/06 *Nonlinear Analysis of a Soil-Drilled Pier System under Static and Dynamic Axial Loading*. Gang Wang and Nicholas Sitar. November 2006.

PEER 2006/05 *Advanced Seismic Assessment Guidelines.* Paolo Bazzurro, C. Allin Cornell, Charles Menun, Maziar Motahari, and Nicolas Luco. September 2006.

PEER 2006/04 *Probabilistic Seismic Evaluation of Reinforced Concrete Structural Components and Systems*. Tae Hyung Lee and Khalid M. Mosalam. August 2006.

PEER 2006/03 *Performance of Lifelines Subjected to Lateral Spreading*. Scott A. Ashford and Teerawut Juirnarongrit. July 2006.

PEER 2006/02 *Pacific Earthquake Engineering Research Center Highway Demonstration Project.* Anne Kiremidjian, James Moore, Yue Yue Fan, Nesrin Basoz, Ozgur Yazali, and Meredith Williams. April 2006.

PEER 2006/01 *Bracing Berkeley. A Guide to Seismic Safety on the UC Berkeley Campus.* Mary C. Comerio, Stephen Tobriner, and Ariane Fehrenkamp. January 2006.

PEER 2005/17 *Earthquake Simulation Tests on Reducing Residual Displacements of Reinforced Concrete Bridges.* Junichi Sakai, Stephen A Mahin, and Andres Espinoza. December 2005.

PEER 2005/16 *Seismic Response and Reliability of Electrical Substation Equipment and Systems.* Junho Song, Armen Der Kiureghian, and Jerome L. Sackman. April 2006.

PEER 2005/15 *CPT-Based Probabilistic Assessment of Seismic Soil Liquefaction Initiation.* R. E. S. Moss, R. B. Seed, R. E. Kayen, J. P. Stewart, and A. Der Kiureghian. April 2006.

PEER 2005/14 *Workshop on Modeling of Nonlinear Cyclic Load-Deformation Behavior of Shallow Foundations.* Bruce L. Kutter, Geoffrey Martin, Tara Hutchinson, Chad Harden, Sivapalan Gajan, and Justin Phalen. March 2006.

PEER 2005/13 *Stochastic Characterization and Decision Bases under Time-Dependent Aftershock Risk in Performance-Based Earthquake Engineering*. Gee Liek Yeo and C. Allin Cornell. July 2005.

PEER 2005/12 *PEER Testbed Study on a Laboratory Building: Exercising Seismic Performance Assessment.* Mary C. Comerio, Editor. November 2005.

PEER 2005/11 *Van Nuys Hotel Building Testbed Report: Exercising Seismic Performance Assessment.* Helmut Krawinkler, Editor. October 2005.

PEER 2005/10 *First NEES/E-Defense Workshop on Collapse Simulation of Reinforced Concrete Building Structures.* September 2005.

PEER 2005/09 *Test Applications of Advanced Seismic Assessment Guidelines.* Joe Maffei, Karl Telleen, Danya Mohr, William Holmes, and Yuki Nakayama. August 2006.

PEER 2005/08 *Damage Accumulation in Lightly Confined Reinforced Concrete Bridge Columns.* R. Tyler Ranf, Jared M. Nelson, Zach Price, Marc O. Eberhard, and John F. Stanton. April 2006.

PEER 2005/07 *Experimental and Analytical Studies on the Seismic Response of Freestanding and Anchored Laboratory Equipment.* Dimitrios Konstantinidis and Nicos Makris. January 2005.

PEER 2005/06 *Global Collapse of Frame Structures under Seismic Excitations*. Luis F. Ibarra and Helmut Krawinkler. September 2005.

PEER 2005//05 *Performance Characterization of Bench- and Shelf-Mounted Equipment.* Samit Ray Chaudhuri and Tara C. Hutchinson. May 2006.

PEER 2005/04 *Numerical Modeling of the Nonlinear Cyclic Response of Shallow Foundations.* Chad Harden, Tara Hutchinson, Geoffrey R. Martin, and Bruce L. Kutter. August 2005.

PEER 2005/03 *A Taxonomy of Building Components for Performance-Based Earthquake Engineering.* Keith A. Porter. September 2005.

PEER 2005/02 *Fragility Basis for California Highway Overpass Bridge Seismic Decision Making*. Kevin R. Mackie and Božidar Stojadinović. June 2005.

PEER 2005/01 *Empirical Characterization of Site Conditions on Strong Ground Motion.* Jonathan P. Stewart, Yoojoong Choi, and Robert W. Graves. June 2005.

PEER 2004/09 *Electrical Substation Equipment Interaction: Experimental Rigid Conductor Studies.* Christopher Stearns and André Filiatrault. February 2005.

PEER 2004/08 *Seismic Qualification and Fragility Testing of Line Break 550-kV Disconnect Switches.* Shakhzod M. Takhirov, Gregory L. Fenves, and Eric Fujisaki. January 2005.

PEER 2004/07 *Ground Motions for Earthquake Simulator Qualification of Electrical Substation Equipment.* Shakhzod M. Takhirov, Gregory L. Fenves, Eric Fujisaki, and Don Clyde. January 2005.

PEER 2004/06 *Performance-Based Regulation and Regulatory Regimes.* Peter J. May and Chris Koski. September 2004.

PEER 2004/05 *Performance-Based Seismic Design Concepts and Implementation: Proceedings of an International Workshop.* Peter Fajfar and Helmut Krawinkler, Editors. September 2004.

PEER 2004/04 *Seismic Performance of an Instrumented Tilt-up Wall Building.* James C. Anderson and Vitelmo V. Bertero. July 2004.

PEER 2004/03 *Evaluation and Application of Concrete Tilt-up Assessment Methodologies.* Timothy Graf and James O. Malley. October 2004.

PEER 2004/02 *Analytical Investigations of New Methods for Reducing Residual Displacements of Reinforced Concrete Bridge Columns.* Junichi Sakai and Stephen A. Mahin. August 2004.

PEER 2004/01 *Seismic Performance of Masonry Buildings and Design Implications.* Kerri Anne Taeko Tokoro, James C. Anderson, and Vitelmo V. Bertero. February 2004.

PEER 2003/18 *Performance Models for Flexural Damage in Reinforced Concrete Columns.* Michael Berry and Marc Eberhard. August 2003.

PEER 2003/17 *Predicting Earthquake Damage in Older Reinforced Concrete Beam-Column Joints.* Catherine Pagni and Laura Lowes. October 2004.

PEER 2003/16 *Seismic Demands for Performance-Based Design of Bridges.* Kevin Mackie and Božidar Stojadinović. August 2003.

PEER 2003/15 *Seismic Demands for Nondeteriorating Frame Structures and Their Dependence on Ground Motions.* Ricardo Antonio Medina and Helmut Krawinkler. May 2004.

PEER 2003/14 *Finite Element Reliability and Sensitivity Methods for Performance-Based Earthquake Engineering*. Terje Haukaas and Armen Der Kiureghian. April 2004.

PEER 2003/13 *Effects of Connection Hysteretic Degradation on the Seismic Behavior of Steel Moment-Resisting Frames.* Janise E. Rodgers and Stephen A. Mahin. March 2004.

PEER 2003/12 *Implementation Manual for the Seismic Protection of Laboratory Contents: Format and Case Studies*. William T. Holmes and Mary C. Comerio. October 2003.

PEER 2003/11 *Fifth U.S.-Japan Workshop on Performance-Based Earthquake Engineering Methodology for Reinforced Concrete Building Structures*. February 2004.

PEER 2003/10 *A Beam-Column Joint Model for Simulating the Earthquake Response of Reinforced Concrete Frames.* Laura N. Lowes, Nilanjan Mitra, and Arash Altoontash. February 2004.

PEER 2003/09 *Sequencing Repairs after an Earthquake: An Economic Approach.* Marco Casari and Simon J. Wilkie. April 2004.

PEER 2003/08 *A Technical Framework for Probability-Based Demand and Capacity Factor Design (DCFD) Seismic Formats*. Fatemeh Jalayer and C. Allin Cornell. November 2003.

PEER 2003/07 *Uncertainty Specification and Propagation for Loss Estimation Using FOSM Methods.* Jack W. Baker and C. Allin Cornell. September 2003.

PEER 2003/06 *Performance of Circular Reinforced Concrete Bridge Columns under Bidirectional Earthquake Loading*. Mahmoud M. Hachem, Stephen A. Mahin, and Jack P. Moehle. February 2003.

PEER 2003/05 *Response Assessment for Building-Specific Loss Estimation*. Eduardo Miranda and Shahram Taghavi. September 2003.

PEER 2003/04 *Experimental Assessment of Columns with Short Lap Splices Subjected to Cyclic Loads*. Murat Melek, John W. Wallace, and Joel Conte. April 2003.

PEER 2003/03 *Probabilistic Response Assessment for Building-Specific Loss Estimation*. Eduardo Miranda and Hesameddin Aslani. September 2003.

PEER 2003/02 *Software Framework for Collaborative Development of Nonlinear Dynamic Analysis Program*. Jun Peng and Kincho H. Law. September 2003.

PEER 2003/01 *Shake Table Tests and Analytical Studies on the Gravity Load Collapse of Reinforced Concrete Frames.* Kenneth John Elwood and Jack P. Moehle. November 2003.

PEER 2002/24 *Performance of Beam to Column Bridge Joints Subjected to a Large Velocity Pulse.* Natalie Gibson, André Filiatrault, and Scott A. Ashford. April 2002.

PEER 2002/23 *Effects of Large Velocity Pulses on Reinforced Concrete Bridge Columns.* Greg L. Orozco and Scott A. Ashford. April 2002.

PEER 2002/22 *Characterization of Large Velocity Pulses for Laboratory Testing.* Kenneth E. Cox and Scott A. Ashford. April 2002.

PEER 2002/21 *Fourth U.S.-Japan Workshop on Performance-Based Earthquake Engineering Methodology for Reinforced Concrete Building Structures*. December 2002.

PEER 2002/20 *Barriers to Adoption and Implementation of PBEE Innovations.* Peter J. May. August 2002.

PEER 2002/19 *Economic-Engineered Integrated Models for Earthquakes: Socioeconomic Impacts.* Peter Gordon, James E. Moore II, and Harry W. Richardson. July 2002.

PEER 2002/18 *Assessment of Reinforced Concrete Building Exterior Joints with Substandard Details.* Chris P. Pantelides, Jon Hansen, Justin Nadauld, and Lawrence D. Reaveley. May 2002.

PEER 2002/17 *Structural Characterization and Seismic Response Analysis of a Highway Overcrossing Equipped with Elastomeric Bearings and Fluid Dampers: A Case Study*. Nicos Makris and Jian Zhang. November 2002.

PEER 2002/16 *Estimation of Uncertainty in Geotechnical Properties for Performance-Based Earthquake Engineering*. Allen L. Jones, Steven L. Kramer, and Pedro Arduino. December 2002.

PEER 2002/15 *Seismic Behavior of Bridge Columns Subjected to Various Loading Patterns*. Asadollah Esmaeily-Gh. and Yan Xiao. December 2002.

PEER 2002/14 *Inelastic Seismic Response of Extended Pile Shaft Supported Bridge Structures.* T.C. Hutchinson, R.W. Boulanger, Y.H. Chai, and I.M. Idriss. December 2002.

PEER 2002/13 *Probabilistic Models and Fragility Estimates for Bridge Components and Systems.* Paolo Gardoni, Armen Der Kiureghian, and Khalid M. Mosalam. June 2002.

PEER 2002/12 *Effects of Fault Dip and Slip Rake on Near-Source Ground Motions: Why Chi-Chi Was a Relatively Mild M7.6 Earthquake*. Brad T. Aagaard, John F. Hall, and Thomas H. Heaton. December 2002.

PEER 2002/11 *Analytical and Experimental Study of Fiber-Reinforced Strip Isolators*. James M. Kelly and Shakhzod M. Takhirov. September 2002.

PEER 2002/10 *Centrifuge Modeling of Settlement and Lateral Spreading with Comparisons to Numerical Analyses***.** Sivapalan Gajan and Bruce L. Kutter. January 2003.

PEER 2002/09 *Documentation and Analysis of Field Case Histories of Seismic Compression during the 1994 Northridge, California, Earthquake*. Jonathan P. Stewart, Patrick M. Smith, Daniel H. Whang, and Jonathan D. Bray. October 2002.

PEER 2002/08 *Component Testing, Stability Analysis and Characterization of Buckling-Restrained Unbonded Braces™*. Cameron Black, Nicos Makris, and Ian Aiken. September 2002.

PEER 2002/07 *Seismic Performance of Pile-Wharf Connections.* Charles W. Roeder, Robert Graff, Jennifer Soderstrom, and Jun Han Yoo. December 2001.

PEER 2002/06 *The Use of Benefit-Cost Analysis for Evaluation of Performance-Based Earthquake Engineering Decisions*. Richard O. Zerbe and Anthony Falit-Baiamonte. September 2001.

PEER 2002/05 *Guidelines, Specifications, and Seismic Performance Characterization of Nonstructural Building Components and Equipment*. André Filiatrault, Constantin Christopoulos, and Christopher Stearns. September 2001.

PEER 2002/04 *Consortium of Organizations for Strong-Motion Observation Systems and the Pacific Earthquake Engineering Research Center Lifelines Program: Invited Workshop on Archiving and Web Dissemination of Geotechnical Data, 4–5 October 2001*. September 2002.

PEER 2002/03 *Investigation of Sensitivity of Building Loss Estimates to Major Uncertain Variables for the Van Nuys Testbed*. Keith A. Porter, James L. Beck, and Rustem V. Shaikhutdinov. August 2002.

PEER 2002/02 *The Third U.S.-Japan Workshop on Performance-Based Earthquake Engineering Methodology for Reinforced Concrete Building Structures*. July 2002.

PEER 2002/01 *Nonstructural Loss Estimation: The UC Berkeley Case Study.* Mary C. Comerio and John C. Stallmeyer. December 2001.

PEER 2001/16 *Statistics of SDF-System Estimate of Roof Displacement for Pushover Analysis of Buildings.* Anil K. Chopra, Rakesh K. Goel, and Chatpan Chintanapakdee. December 2001.

PEER 2001/15 *Damage to Bridges during the 2001 Nisqually Earthquake.* R. Tyler Ranf, Marc O. Eberhard, and Michael P. Berry. November 2001.

PEER 2001/14 *Rocking Response of Equipment Anchored to a Base Foundation.* Nicos Makris and Cameron J. Black. September 2001.

PEER 2001/13 *Modeling Soil Liquefaction Hazards for Performance-Based Earthquake Engineering*. Steven L. Kramer and Ahmed-W. Elgamal. February 2001.

PEER 2001/12 *Development of Geotechnical Capabilities in OpenSees*. Boris Jeremić. September 2001.

PEER 2001/11 *Analytical and Experimental Study of Fiber-Reinforced Elastomeric Isolators*. James M. Kelly and Shakhzod M. Takhirov. September 2001.

PEER 2001/10 *Amplification Factors for Spectral Acceleration in Active Regions.* Jonathan P. Stewart, Andrew H. Liu, Yoojoong Choi, and Mehmet B. Baturay. December 2001.

PEER 2001/09 *Ground Motion Evaluation Procedures for Performance-Based Design.* Jonathan P. Stewart, Shyh-Jeng Chiou, Jonathan D. Bray, Robert W. Graves, Paul G. Somerville, and Norman A. Abrahamson. September 2001.

PEER 2001/08 *Experimental and Computational Evaluation of Reinforced Concrete Bridge Beam-Column Connections for Seismic Performance*. Clay J. Naito, Jack P. Moehle, and Khalid M. Mosalam. November 2001.

PEER 2001/07 *The Rocking Spectrum and the Shortcomings of Design Guidelines.* Nicos Makris and Dimitrios Konstantinidis. August 2001.

PEER 2001/06 *Development of an Electrical Substation Equipment Performance Database for Evaluation of Equipment Fragilities*. Thalia Agnanos. April 1999.

PEER 2001/05 *Stiffness Analysis of Fiber-Reinforced Elastomeric Isolators.* Hsiang-Chuan Tsai and James M. Kelly. May 2001.

PEER 2001/04 *Organizational and Societal Considerations for Performance-Based Earthquake Engineering*. Peter J. May. April 2001.

PEER 2001/03 *A Modal Pushover Analysis Procedure to Estimate Seismic Demands for Buildings: Theory and Preliminary Evaluation*. Anil K. Chopra and Rakesh K. Goel. January 2001.

PEER 2001/02 *Seismic Response Analysis of Highway Overcrossings Including Soil-Structure Interaction*. Jian Zhang and Nicos Makris. March 2001.

PEER 2001/01 *Experimental Study of Large Seismic Steel Beam-to-Column Connections.* Egor P. Popov and Shakhzod M. Takhirov. November 2000.

PEER 2000/10 *The Second U.S.-Japan Workshop on Performance-Based Earthquake Engineering Methodology for Reinforced Concrete Building Structures*. March 2000.

PEER 2000/09 *Structural Engineering Reconnaissance of the August 17, 1999 Earthquake: Kocaeli (Izmit), Turkey*. Halil Sezen, Kenneth J. Elwood, Andrew S. Whittaker, Khalid Mosalam, John J. Wallace, and John F. Stanton. December 2000.

PEER 2000/08 *Behavior of Reinforced Concrete Bridge Columns Having Varying Aspect Ratios and Varying Lengths of Confinement*. Anthony J. Calderone, Dawn E. Lehman, and Jack P. Moehle. January 2001.

PEER 2000/07 *Cover-Plate and Flange-Plate Reinforced Steel Moment-Resisting Connections.* Taejin Kim, Andrew S. Whittaker, Amir S. Gilani, Vitelmo V. Bertero, and Shakhzod M. Takhirov. September 2000.

PEER 2000/06 *Seismic Evaluation and Analysis of 230-kV Disconnect Switches.* Amir S. J. Gilani, Andrew S. Whittaker, Gregory L. Fenves, Chun-Hao Chen, Henry Ho, and Eric Fujisaki. July 2000.

PEER 2000/05 *Performance-Based Evaluation of Exterior Reinforced Concrete Building Joints for Seismic Excitation*. Chandra Clyde, Chris P. Pantelides, and Lawrence D. Reaveley. July 2000.

PEER 2000/04 *An Evaluation of Seismic Energy Demand: An Attenuation Approach*. Chung-Che Chou and Chia-Ming Uang. July 1999.

PEER 2000/03 *Framing Earthquake Retrofitting Decisions: The Case of Hillside Homes in Los Angeles.* Detlof von Winterfeldt, Nels Roselund, and Alicia Kitsuse. March 2000.

PEER 2000/02 *U.S.-Japan Workshop on the Effects of Near-Field Earthquake Shaking*. Andrew Whittaker, Editor. July 2000.

PEER 2000/01 *Further Studies on Seismic Interaction in Interconnected Electrical Substation Equipment.* Armen Der Kiureghian, Kee-Jeung Hong, and Jerome L. Sackman. November 1999.

PEER 1999/14 *Seismic Evaluation and Retrofit of 230-kV Porcelain Transformer Bushings*. Amir S. Gilani, Andrew S. Whittaker, Gregory L. Fenves, and Eric Fujisaki. December 1999.

PEER 1999/13 *Building Vulnerability Studies: Modeling and Evaluation of Tilt-up and Steel Reinforced Concrete Buildings*. John W. Wallace, Jonathan P. Stewart, and Andrew S. Whittaker, Editors. December 1999.

PEER 1999/12 *Rehabilitation of Nonductile RC Frame Building Using Encasement Plates and Energy-Dissipating Devices*. Mehrdad Sasani, Vitelmo V. Bertero, James C. Anderson. December 1999.

PEER 1999/11 *Performance Evaluation Database for Concrete Bridge Components and Systems under Simulated Seismic Loads*. Yael D. Hose and Frieder Seible. November 1999.

PEER 1999/10 *U.S.-Japan Workshop on Performance-Based Earthquake Engineering Methodology for Reinforced Concrete Building Structures*. December 1999.

PEER 1999/09 *Performance Improvement of Long Period Building Structures Subjected to Severe Pulse-Type Ground Motions*. James C. Anderson, Vitelmo V. Bertero, and Raul Bertero. October 1999.

PEER 1999/08 *Envelopes for Seismic Response Vectors.* Charles Menun and Armen Der Kiureghian. July 1999.

PEER 1999/07 *Documentation of Strengths and Weaknesses of Current Computer Analysis Methods for Seismic Performance of Reinforced Concrete Members*. William F. Cofer. November 1999.

PEER 1999/06 *Rocking Response and Overturning of Anchored Equipment under Seismic Excitations*. Nicos Makris and Jian Zhang. November 1999.

PEER 1999/05 *Seismic Evaluation of 550 kV Porcelain Transformer Bushings.* Amir S. Gilani, Andrew S. Whittaker, Gregory L. Fenves, and Eric Fujisaki. October 1999.

PEER 1999/04 *Adoption and Enforcement of Earthquake Risk-Reduction Measures.* Peter J. May, Raymond J. Burby, T. Jens Feeley, and Robert Wood. August 1999.

PEER 1999/03 *Task 3 Characterization of Site Response General Site Categories*. Adrian Rodriguez-Marek, Jonathan D. Bray and Norman Abrahamson. February 1999.

PEER 1999/02 *Capacity-Demand-Diagram Methods for Estimating Seismic Deformation of Inelastic Structures: SDF Systems*. Anil K. Chopra and Rakesh Goel. April 1999.

PEER 1999/01 *Interaction in Interconnected Electrical Substation Equipment Subjected to Earthquake Ground Motions*. Armen Der Kiureghian, Jerome L. Sackman, and Kee-Jeung Hong. February 1999.

PEER 1998/08 *Behavior and Failure Analysis of a Multiple-Frame Highway Bridge in the 1994 Northridge Earthquake*. Gregory L. Fenves and Michael Ellery. December 1998.

PEER 1998/07 *Empirical Evaluation of Inertial Soil-Structure Interaction Effects.* Jonathan P. Stewart, Raymond B. Seed, and Gregory L. Fenves. November 1998.

PEER 1998/06 *Effect of Damping Mechanisms on the Response of Seismic Isolated Structures*. Nicos Makris and Shih-Po Chang. November 1998.

PEER 1998/05 *Rocking Response and Overturning of Equipment under Horizontal Pulse-Type Motions*. Nicos Makris and Yiannis Roussos. October 1998.

PEER 1998/04 *Pacific Earthquake Engineering Research Invitational Workshop Proceedings, May 14–15, 1998: Defining the Links between Planning, Policy Analysis, Economics and Earthquake Engineering*. Mary Comerio and Peter Gordon. September 1998.

PEER 1998/03 *Repair/Upgrade Procedures for Welded Beam to Column Connections*. James C. Anderson and Xiaojing Duan. May 1998.

PEER 1998/02 *Seismic Evaluation of 196 kV Porcelain Transformer Bushings.* Amir S. Gilani, Juan W. Chavez, Gregory L. Fenves, and Andrew S. Whittaker. May 1998.

PEER 1998/01 *Seismic Performance of Well-Confined Concrete Bridge Columns.* Dawn E. Lehman and Jack P. Moehle. December 2000.

PEER REPORTS: ONE HUNDRED SERIES

The following PEER reports are available by Internet only at http://peer.berkeley.edu/publications/peer_reports_complete.html.

PEER 2012/103 *Performance-Based Seismic Demand Assessment of Concentrically Braced Steel Frame Buildings.* Chui-Hsin Chen and Stephen A. Mahin. December 2012.

PEER 2012/102 *Procedure to Restart an Interrupted Hybrid Simulation: Addendum to PEER Report 2010/103.* Vesna Terzic and Bozidar Stojadinovic. October 2012.

PEER 2012/101 *Mechanics of Fiber Reinforced Bearings.* James M. Kelly and Andrea Calabrese. February 2012.

PEER 2011/107 *Nonlinear Site Response and Seismic Compression at Vertical Array Strongly Shaken by 2007 Niigata-ken Chuetsu-oki Earthquake.* Eric Yee, Jonathan P. Stewart, and Kohji Tokimatsu. December 2011.

PEER 2011/106 *Self Compacting Hybrid Fiber Reinforced Concrete Composites for Bridge Columns.* Pardeep Kumar, Gabriel Jen, William Trono, Marios Panagiotou, and Claudia Ostertag. September 2011.

PEER 2011/105 *Stochastic Dynamic Analysis of Bridges Subjected to Spacially Varying Ground Motions.* Katerina Konakli and Armen Der Kiureghian. August 2011.

PEER 2011/104 *Design and Instrumentation of the 2010 E-Defense Four-Story Reinforced Concrete and Post-Tensioned Concrete Buildings.* Takuya Nagae, Kenichi Tahara, Taizo Matsumori, Hitoshi Shiohara, Toshimi Kabeyasawa, Susumu Kono, Minehiro Nishiyama (Japanese Research Team) and John Wallace, Wassim Ghannoum, Jack Moehle, Richard Sause, Wesley Keller, Zeynep Tuna (U.S. Research Team). June 2011.

PEER 2011/103 *In-Situ Monitoring of the Force Output of Fluid Dampers: Experimental Investigation.* Dimitrios Konstantinidis, James M. Kelly, and Nicos Makris. April 2011.

PEER 2011/102 *Ground-Motion Prediction Equations 1964–2010.* John Douglas. April 2011.

PEER 2011/101 *Report of the Eighth Planning Meeting of NEES/E-Defense Collaborative Research on Earthquake Engineering.* Convened by the Hyogo Earthquake Engineering Research Center (NIED), NEES Consortium, Inc. February 2011.

PEER 2010/111 *Modeling and Acceptance Criteria for Seismic Design and Analysis of Tall Buildings.* Task 7 Report for the Tall Buildings Initiative - Published jointly by the Applied Technology Council. October 2010.

PEER 2010/110 *Seismic Performance Assessment and Probabilistic Repair Cost Analysis of Precast Concrete Cladding Systems for Multistory Buildlings.* Jeffrey P. Hunt and Božidar Stojadinovic. November 2010.

PEER 2010/109 *Report of the Seventh Joint Planning Meeting of NEES/E-Defense Collaboration on Earthquake Engineering. Held at the E-Defense, Miki, and Shin-Kobe, Japan, September 18–19, 2009.* August 2010.

PEER 2010/108 *Probabilistic Tsunami Hazard in California.* Hong Kie Thio, Paul Somerville, and Jascha Polet, preparers. October 2010.

PEER 2010/107 *Performance and Reliability of Exposed Column Base Plate Connections for Steel Moment-Resisting Frames.* Ady Aviram, Božidar Stojadinovic, and Armen Der Kiureghian. August 2010.

PEER 2010/106 *Verification of Probabilistic Seismic Hazard Analysis Computer Programs.* Patricia Thomas, Ivan Wong, and Norman Abrahamson. May 2010.

PEER 2010/105 *Structural Engineering Reconnaissance of the April 6, 2009, Abruzzo, Italy, Earthquake, and Lessons Learned.* M. Selim Günay and Khalid M. Mosalam. April 2010.

PEER 2010/104 *Simulating the Inelastic Seismic Behavior of Steel Braced Frames, Including the Effects of Low-Cycle Fatigue.* Yuli Huang and Stephen A. Mahin. April 2010.

PEER 2010/103 *Post-Earthquake Traffic Capacity of Modern Bridges in California.* Vesna Terzic and Božidar Stojadinović. March 2010.

PEER 2010/102 *Analysis of Cumulative Absolute Velocity (CAV) and JMA Instrumental Seismic Intensity (I_{JMA}) Using the PEER–NGA Strong Motion Database.* Kenneth W. Campbell and Yousef Bozorgnia. February 2010.

PEER 2010/101 *Rocking Response of Bridges on Shallow Foundations.* Jose A. Ugalde, Bruce L. Kutter, and Boris Jeremic. April 2010.

PEER 2009/109 *Simulation and Performance-Based Earthquake Engineering Assessment of Self-Centering Post-Tensioned Concrete Bridge Systems.* Won K. Lee and Sarah L. Billington. December 2009.

PEER 2009/108 *PEER Lifelines Geotechnical Virtual Data Center.* J. Carl Stepp, Daniel J. Ponti, Loren L. Turner, Jennifer N. Swift, Sean Devlin, Yang Zhu, Jean Benoit, and John Bobbitt. September 2009.

PEER 2009/107 *Experimental and Computational Evaluation of Current and Innovative In-Span Hinge Details in Reinforced Concrete Box-Girder Bridges: Part 2: Post-Test Analysis and Design Recommendations.* Matias A. Hube and Khalid M. Mosalam. December 2009.

PEER 2009/106 *Shear Strength Models of Exterior Beam-Column Joints without Transverse Reinforcement.* Sangjoon Park and Khalid M. Mosalam. November 2009.

PEER 2009/105 *Reduced Uncertainty of Ground Motion Prediction Equations through Bayesian Variance Analysis.* Robb Eric S. Moss. November 2009.

PEER 2009/104 *Advanced Implementation of Hybrid Simulation.* Andreas H. Schellenberg, Stephen A. Mahin, Gregory L. Fenves. November 2009.

PEER 2009/103 *Performance Evaluation of Innovative Steel Braced Frames.* T. Y. Yang, Jack P. Moehle, and Božidar Stojadinovic. August 2009.

PEER 2009/102 *Reinvestigation of Liquefaction and Nonliquefaction Case Histories from the 1976 Tangshan Earthquake.* Robb Eric Moss, Robert E. Kayen, Liyuan Tong, Songyu Liu, Guojun Cai, and Jiaer Wu. August 2009.

PEER 2009/101 *Report of the First Joint Planning Meeting for the Second Phase of NEES/E-Defense Collaborative Research on Earthquake Engineering.* Stephen A. Mahin et al. July 2009.

PEER 2008/104 *Experimental and Analytical Study of the Seismic Performance of Retaining Structures.* Linda Al Atik and Nicholas Sitar. January 2009.

PEER 2008/103 *Experimental and Computational Evaluation of Current and Innovative In-Span Hinge Details in Reinforced Concrete Box-Girder Bridges. Part 1: Experimental Findings and Pre-Test Analysis.* Matias A. Hube and Khalid M. Mosalam. January 2009.

PEER 2008/102 *Modeling of Unreinforced Masonry Infill Walls Considering In-Plane and Out-of-Plane Interaction.* Stephen Kadysiewski and Khalid M. Mosalam. January 2009.

PEER 2008/101 *Seismic Performance Objectives for Tall Buildings.* William T. Holmes, Charles Kircher, William Petak, and Nabih Youssef. August 2008.

PEER 2007/101 *Generalized Hybrid Simulation Framework for Structural Systems Subjected to Seismic Loading*. Tarek Elkhoraibi and Khalid M. Mosalam. July 2007.

PEER 2007/100 *Seismic Evaluation of Reinforced Concrete Buildings Including Effects of Masonry Infill Walls*. Alidad Hashemi and Khalid M. Mosalam. July 2007.

The Pacifi c Earthquake Engineering Research Center (PEER) is a multi-institutional research and education center with headquarters at the University of California, Berkeley. Investigators from over 20 universities, several consulting companies, and researchers at various state and federal government agencies contribute to research programs focused on performance-based earthquake engineering.

These research programs aim to identify and reduce the risks from major earthquakes to life safety and to the economy by including research in a wide variety of disciplines including structural and geotechnical engineering, geology/seismology, lifelines, transportation, architecture, economics, risk management, and public policy.

PEER is supported by federal, state, local, and regional agencies, together with industry partners.

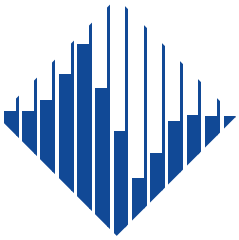

PEER Core Institutions

University of California, Berkeley (Lead Institution)
California Institute of Technology
Oregon State University
Stanford University
University of California, Davis
University of California, Irvine
University of California, Los Angeles
University of California, San Diego
University of Nevada, Reno
University of Southern California
University of Washington

PEER reports can be ordered at https://peer.berkeley.edu/peer-reports or by contacting

Pacific Earthquake Engineering Research Center
University of California, Berkeley
325 Davis Hall, Mail Code 1792
Berkeley, CA 94720-1792
Tel: 510-642-3437
Email: peer_center@berkeley.edu

ISSN 2770-8314
https://doi.org/10.55461/LTMU9309